REPORT SERIES IN GEOPHYSICS
N:o 80 (2019)

IMPROVED UNDERSTANDING OF FACTORS AFFECTING URBAN HYDROLOGICAL CYCLE

TOM KOKKONEN

Institute for Atmospheric and Earth System Research / Physics
Faculty of Science
University of Helsinki
Helsinki, Finland

Academic dissertation

To be presented, with the permission of the Faculty of Science of the University of Helsinki, for public criticism in auditorium B123, Pietari Kalmin katu 5, on March 22nd, 2019, at 12 o'clock noon.

Helsinki 2019

Author's Address: Institute for Atmospheric and Earth System Research / Physics
P.O. Box 68
FI-00014 University of Helsinki
tom.kokkonen@helsinki.fi

Supervisors: Associate Professor Leena Järvi, Ph.D.
Institute for Atmospheric and Earth System Research / Physics &
Helsinki Institute of Sustainability Science
University of Helsinki

Emeritus Professor Matti Leppäranta, Ph.D.
Institute for Atmospheric and Earth System Research / Physics
University of Helsinki

Reviewers: Head of group Carl Fortelius, Ph.D.
Numerical weather prediction
Finnish Meteorological Institute

Docent Samuli Launiainen, Ph.D.
Natural Resources Institute Finland

Opponent: Professor Guangheng Ni, Ph.D.
Department of Hydraulic Engineering
Tsinghua University

ISBN 978-951-51-4979-4 (printed version)
ISSN 0355-8630
Helsinki 2019
Yliopistopaino

ISBN 978-951-51-4980-0 (pdf version)
http://ethesis.helsinki.fi
Helsinki 2019
Helsingin yliopiston verkkojulkaisut

Cover picture: View from the measurement station at the Hotel Torni.

Acknowledgements

This research was carried out in the Institute for Atmospheric and Earth System Research (formerly Division of Atmospheric Sciences) of the University of Helsinki. I acknowledge Maj and Tor Nessling Foundation (grant 201400502, 201500273 and 201600458) and Maa- ja vesitekniikan tuki ry (grant 36663) for the funding of this thesis. I want to express my gratitude for the Director of the Institute for Atmospheric and Earth System Research, Academician, Professor Markku Kulmala for providing the inspiring working environment in one of the leading research groups in atmospheric sciences. I want to also thank the urban meteorology and geophysics groups for all the discussions and support.

During my studies I have had great mentoring from several senior researchers, but I want to thank especially my thesis supervisors Associate Professor Leena Järvi and Emeritus Professor Matti Leppäranta. I want to thank all my co-authors, but I would like to acknowledge especially Professor Sue Grimmond who has been a vital asset in all of my first author papers in this thesis. Further, I want to thank all the other colleagues from micromet and BUCT groups.

Finally I want to express my deepest gratitudes for my whole family who have supported me greatly throughout the whole PhD project. I want to thank especially my wife Tiina and my two daughters Sonja and Olivia. This would not have been possible without your support.

Tom Valtteri Kokkonen
University of Helsinki, 2018

Abstract

The processes related to urban development (urbanisation, densification, irrigation and worsened air quality) are assumed to affect the urban hydrological cycle, but little is known about the impact of the individual processes. One of the reasons for the knowledge gaps is the lack of measurements for the needed resolution or for the period of interest. Reanalysis products can provide the needed data, but those have not been evaluated in urban areas. Furthermore, model evaluation is commonly made against eddy covariance (EC) measurements, but little is known of the uncertainties related to often non-ideal instrument location at urban areas.

To answer the uncertainties in urban hydrological cycle, Surface Urban Energy and Water Balance Scheme (SUEWS) forced with the WATCH Forcing Data is used. The analyses are performed in cities located in different climate conditions (Vancouver, London and Beijing) and above varying urban land covers (dense city centre and suburban areas). To understand better the uncertainties related to model evaluation, uncertainties of EC method are analysed using two identical EC systems at the same level close to each other in central Helsinki.

The most crucial reanalysis variables to correct are precipitation due to coarse spatial resolution and the incoming solar radiation due to haze. SUEWS performs well when forced with corrected WATCH data, which allows detailed analysis of urban hydrological cycle. The irrigation has the dominant effect over densification and urbanisation on suburban hydrological cycle. The densification increases the runoff as much as the initial urbanisation, even though the increase of impervious surfaces is much smaller. The haze decreases evaporation which increases runoff and soil infiltration especially at smaller daily precipitation totals. This is expected to flush pollutants from surfaces and increase the pollutant loads of urban waters.

After the post-processing of the EC data, systematic uncertainties in latent heat flux originating from a single-point observation above dense city centre due to removal of large fraction of wind disturbed data are only 8%. Thus, useful and representative EC observations can be obtained from urban areas, despite the errors induced by the non-ideal location.

The results of this thesis answer the uncertainties in urban hydrological cycle by bringing new knowledge of the dominant factors in the urban water balance and the representativeness of reanalysis data in urban areas. The results can help urban planners to design sustainable cities being able to mitigate and adapt to the common problems in urban hydrology.

Keywords: eddy covariance, modelling uncertainty, reanalysis data, SUEWS, urban hydrology, urban climate, WATCH

Contents

List of publications

This thesis consists of an introductory review, followed by 4 research articles. **Papers I and IV** are reprinted under the Creative Commons Attribution 4.0 License, **Paper II** is reprinted with permission from Elsevier and **Paper III** is reprinted with license from John Wiley and Sons (license number 4464150530494). In the introductory part, these papers are cited according to their roman numerals.

I Järvi, L., Rannik, Ü., Kokkonen, T. V., Kurppa, M., Karppinen, A., Kouznetsov, R. D., Rantala, P., Vesala, T., and Wood, C. R. (2018). Uncertainty of eddy covariance flux measurements over an urban area based on two towers, *Atmos. Meas. Tech.*, 11(10):5421–5438, doi:10.5194/amt-2018-89.

II Kokkonen, T. V., Grimmond, C. S. B., Räty, O., Ward, H. C., Christen, A., Oke, T. R., Kotthaus, S., and Järvi, L. (2018). Sensitivity of Surface Urban Energy and Water Balance Scheme (SUEWS) to downscaling of reanalysis forcing data, *Urban Climate*, 23:36–52, doi:10.1016/j.uclim.2017.05.001.

III Kokkonen, T. V., Grimmond, C. S. B., Christen, A., Oke, T. R., and Järvi, L. (2018). Changes to the water balance over a century of urban development in two neighborhoods: Vancouver, Canada, *Water Resour. Res.*, 54(9):6625–6642, doi:10.1029/2017WR022445.

IV Kokkonen, T. V., Grimmond, C. S. B., Murto, S., Liu, H. Z., Sundström, A.-M., and Järvi, L. (2019). Simulation of the radiative effect of haze on urban hydrological cycle using reanalysis data in Beijing, *Atmos. Chem. Phys. Discuss.*, doi:10.5194/acp-2018-1226.

1 Introduction

1.1 Motivation

Increasing number of people live in urban environments (United Nations, 2014) and are exposed to cities' local climate. Urban areas commonly have high concentration of atmospheric pollutants, increased heat stress, decreased evaporation and increased risk of flooding compared to surrounding natural areas. All these phenomena influence human well-being and one of the main aims of urban planning is to minimize their negative effects. Only with research-based knowledge, urban planners are able to design sustainable cities that can effectively adapt and mitigate to the problems related to urban climate (Baklanov et al., 2018).

In addition to human comfort effects, many of the local climate phenomena have economic effects and health costs. Especially flooding can cause massive economical costs. For example, only in the European Union the annual economical losses due to flooding are estimated to be 4.9 billion euros between years 2000–2012 (Jongman et al., 2014). Furthermore in the future, increased risk of flooding caused by increased heavy rainfall events due to climate change (Lenderink and van Meijgaard, 2008; Min et al., 2011; O'Gorman and Schneider, 2009) and changes in land use (Rodriguez et al., 2003; Valtanen et al., 2014) is expected. The primary impact of urbanization comes from the increase of impervious surfaces. Thus, the accurate determination of cover fraction of impervious surfaces is critical in urban hydrological modelling (Ramamurthy and Bou-Zeid, 2014; Tokarczyk et al., 2015). A secondary effect of urbanization on the water balance is the loss of vegetation reducing evapotranspiration. These changes induced by urbanization decrease water storage in soil as well as evaporation and therefore more of the available water will be directed to surface runoff (Rodriguez et al., 2003). However, the impact of increased impervious surfaces to runoff due to further densification of already existing urban structures (e.g. building of garages, terraces and driveways) has still remained unstudied. Thirdly, garden irrigation can have a substantial effect on the urban water balance especially in areas with many gardens (e.g. suburban areas) (Best and Grimmond, 2016; Grimmond and Oke, 1986; Demuzere et al., 2014; Mitchell et al., 2001b, 2003; Oke et al., 2017; Templeton et al., 2018). This effect could be reduced by imposing regulations to garden irrigation. The detailed impacts of garden irrigation regulations to urban hydrological cycle on different years with varying meteorological conditions have not yet been studied, since previous studies have focused on the short-term effects on the hydrological conditions (e.g. Demuzere et al., 2014) or the cooling effect (e.g. Gober et al., 2009).

The exposure to atmospheric pollution causes up to 4 million premature deaths per year worldwide (Cohen et al., 2017; Lelieveld et al., 2015). In addition to health problems, air pollution also enhances climate change (Molina and Molina, 2004). The aerosols in air attenuate the incoming solar radiation and therefore reduce surface energy availability and turbulent heat fluxes (Kajino et al., 2017; Petäjä et al., 2016). With less energy available at the surface also evaporation decreases. The increasing atmospheric stability due to absorption of solar radiation by the aerosols can also lead to an increased risk of heavy rainfall increasing substantially the risk of flooding (Fan et al., 2015). In addition, even small rainfall totals flush pollutants from contaminated surfaces to surface runoff water (Yufen et al., 2008). Therefore it is important to understand the impact of air quality on hydrological cycle, on runoff in particular. In recent years the air quality in urban areas has been deteriorating and especially in developing countries the air pollution is a significant problem (Kan et al., 2012; Kulmala, 2015; Mayer, 1999; Molina and Molina, 2004). With continuing economical growth the air pollution is estimated to increase even further (Zhao et al., 2013). Even though important advances have been made in the past, new studies are needed to increase understanding of interactions between the air quality and regional and global climate and the hydrological cycle (Baklanov et al., 2018).

Modelling of urban water balance and the effects of urbanization and atmospheric pollution are needed in different climate conditions and city structures (e.g. city centre and suburban areas) to be able to properly understand the problems in urban hydrometeorology (here after simply hydrology). In order to make detailed modelling of the urban hydrological cycle, location-specific meteorological observations with high temporal resolution are needed to force the urban land surface and hydrological models (Kanamitsu and Kanamaru, 2007; Wood et al., 2004). Although more urban observational sites have been installed (Barlow, 2014; Grimmond, 2006), direct observations of required variables to force urban models are rare (e.g. Kulmala, 2018). Observations are typically limited to individual sites in a few cities and do not address the diversity of urban areas globally. Therefore, location-specific observations from urban areas of all the needed variables in high enough resolution are lacking especially in the developing countries (Grimmond et al., 2010a; IPCC, 2014; World Meteorological Organization, 2015).

Here global reanalysis products can help by providing the essential variables for hydrological modelling in the areas where needed observations are unavailable, have too coarse temporal resolution or the observations lack from the period of interest. Reanalysis data are generated by using single consistent data assimilation method combining meteorological models and a large amount of remote sensing and ground based observations creating consistent time series of multiple meteorological variables spanning an extended period. Although there are multiple reanalysis products available (e.g. ERA-Interim (Dee et al., 2011), JRA-55 (Kobayashi et al., 2015), MERRA (Rienecker et al., 2011), NCEP (Kalnay et al., 1996), WFDEI (Weedon et al., 2014)), the spatial resolution is typically coarse (e.g. 0.5°). Therefore downscaling is needed prior to use for local scale urban hydrological modelling (Bastola and Misra, 2014; Fowler et al., 2007; Wilby et al., 2000). However, the reanalysis products have not yet been properly evaluated for hydrological modelling at a local scale in urban environments especially at the highly polluted cities in developing countries, since most of the previous studies focus on urban heat island phenomena or larger scale hydrology (e.g. Früh et al., 2011; Gooré Bi et al., 2017; Lemonsu et al., 2013).

Another issue is related to the evaluation of hydrological models. The eddy covariance (EC) technique is the most direct method to measure the exchange between the surface and the atmosphere and is commonly used for evaluation of land surface models (Grimmond et al., 2010b, 2011). Even though surface fluxes describe only certain parts of land surface models, good correspondence between modelled and measured heat fluxes also indicate smaller uncertainties in the other components of water and energy balances which are commonly more challenging to measure. However, choosing an ideal location for EC observations in urban areas is also challenging due to the heterogeneity of urban surfaces and the limitations of EC setup placement due to logistical and safety restrictions. Thus flow distortion by adjacent obstacles or the setup itself is especially common in urban environments (Barlow et al., 2011). In the past, the two-tower approach has been used to estimate the uncertainties of EC technique in natural environments (Hollinger and Richardson, 2005; Kessomkiat et al., 2013), whereas the approach has not yet been used in urban areas.

1.2 Objectives

This thesis aims to bring new knowledge in using downscaled reanalysis data in local scale urban hydrological modelling and to understand the dominant factors in the urban hydrological cycle. In addition, this thesis aims to improve understanding of the uncertainties in urban EC observations that are commonly used to evaluate the model performance. The following main questions will be addressed:

- What are the uncertainties in EC measurements commonly used to evaluate urban land surface models? **Paper I**
- How well reanalysis products can be used as forcing data in urban hydrological modelling and which variables are the most important to be corrected? **Papers II and IV**
- What are the relative importance and effects of urbanization, densification and irrigation on local scale hydrological cycle? **Paper III**
- How does air pollution modify the local urban hydrological cycle? **Paper IV**

In order to answer these questions, the WATCH reanalysis data (Weedon et al., 2011, 2014) are evaluated in multiple urban areas and corrections developed for the essential variables. These corrected reanalysis datasets are then used as meteorological forcing for the Surface Urban Energy and Water Balance Scheme (SUEWS; Järvi et al., 2011; Ward et al., 2016) to model water balance in a variety of urban structures and climate conditions. In addition, the uncertainties in urban EC measurements are identified in central Helsinki.

2 Surface–atmosphere interactions

2.1 Surface energy and water balance

The surface energy balance is the fundamental starting point for understanding, analysing and modelling the urban surface microclimates and the atmospheric boundary layer. It describes the net result of energy exchanges by radiation, convection and conduction between the urban surface and the atmosphere. The surface energy balance is an assessment of transfer and storage of energy, based on conservation of energy, between an urban system and atmosphere as well as within that system (Oke, 1988). The urban surface energy balances can be written for individual facets (roofs, walls, roads, vegetation etc.)(Anandakumar, 1999; Arnfield, 2003; Asaeda and Ca, 1993; Oke, 1979), which can be a suitable approach when interested in microscale (10^{-2} to 10^3 m) phenomena. However, in complete urban environments in local scale (10^2 to 5×10^4 m) or mesoscale (10^4 to 2×10^5 m), where multiple facets are linked together forming larger urban units (street canyons, city blocks, neighbourhoods) it becomes impractical to deal with individual surfaces. Instead the urban surface energy balance is commonly determined for a larger volume which represents the whole ecosystem of the urban unit with energy sources (Arnfield, 2003; Grimmond et al., 1991; Kalanda et al., 1980; Oke, 1987, 1988; Oke et al., 2017). The urban surface energy balance for such a volume can be written as (Oke, 1987)

$$Q^* + Q_F = Q_E + Q_H + \Delta Q_S, \quad [\mathrm{W\ m^{-2}}] \tag{1}$$

where Q^* is the net all-wave radiation, Q_F is the anthropogenic heat flux, Q_E is the latent heat flux, Q_H is the sensible heat flux and ΔQ_S is the net storage heat flux (Figure 1a).

The water balance, which is the focus of this thesis, is linked to energy balance through evaporation ($Q_E = L_v E$; L_v is the latent heat of vaporization and E is evapotranspiration, here after simply evaporation). The surface water balance is easier to determine and make observations for natural catchments as it is the net result of precipitation, evaporation, runoff and in/outflowing streams govern mainly by the topographic irregularities and gravity. However, in urban environment human activities and artificial water sources and sinks make the determination of the water balance more complicated. For example artificial pipe networks leading water in and out of the system as

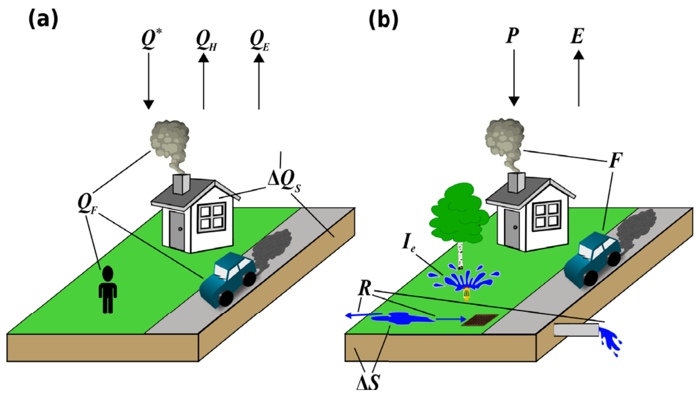

Figure 1: Schematic illustration of urban surface (a) energy and (b) water balances. Q^* is the net all-wave radiation, Q_F is the anthropogenic heat flux, Q_E is the latent heat flux, Q_H is the sensible heat flux, ΔQ_S is the net storage heat flux, P is precipitation, I_e is the net result of external piped water network, F is the anthropogenic water emission, R is runoff and ΔS is the net change in surface and soil water storages. Modified after Oke (1987).

well as clearing of the snow from the catchment area have to be taken into account. In addition, significant amount of anthropogenic water emissions can be induced by traffic, industrial processes and cooling systems (e.g. Moriwaki et al., 2008). A definition of urban catchment is not straightforward because it often does not have a well defined perimeter, nor is the water channelled to a single basin exit. Therefore it is more realistic to refer to urban hydrologic units (Oke et al., 2017), which have multiple natural and anthropogenic inlets and outlets. Thus the urban surface water balance for a single urban neighbourhood as a hydrologic unit applies to a volume, similar to energy balance, and can be written as (Grimmond et al., 1986)

$$P + I_e + F = E + R + \Delta S, \quad [\text{mm h}^{-1}] \tag{2}$$

where P is precipitation, I_e is the net result of external piped water network, F is the anthropogenic water emission, R is runoff and ΔS is the net change in surface and soil water storages (Figure 1b).

The evaporation for urban areas can be calculated using the Penman-Monteith equation (Monteith, 1965; Penman, 1948) modified for urban environments (Grimmond and Oke, 1991):

$$Q_E = \frac{s(Q^* + Q_F - \Delta Q_S) + c_p \rho V / r_a}{s + \gamma(1 + r_s/r_a)}, \tag{3}$$

where s is the slope of the saturation vapour pressure curve, c_p is the specific heat capacity, ρ is the density of air, V is the vapour pressure deficit of air, γ is the psychometric constant, r_a and r_s are aerodynamic and surface resistances, respectively.

Atmospheric pollution modifies the urban energy and water balances by decreasing solar radiation at the surface reducing surface energy availability and sensible and latent heat fluxes (Kajino et al., 2017; Petäjä et al., 2016). The polluted layer absorbs the incoming solar radiation and changes the vertical temperature profile leading to an increased stability and therefore the boundary layer height is reduced (Petäjä et al., 2016).

2.2 Eddy covariance technique

Observations are in a central role in the analyses of urban climate effects and understanding of the processes responsible. Given the growth of cities, in number and size, the need for high resolution long-term observations in urban areas is probably greater now than ever (Kulmala, 2018).

EC technique is the most direct way to measure the two turbulent terms of the energy balance, Q_H and Q_E. The measurement of exchanges of heat, mass and momentum between a flat, horizontally homogeneous surface and the atmosphere using the EC technique was proposed by Montgomery (1948), Swinbank (1951) and Obukhov (1951). However, instrumentation limitations restricted early implementation of this approach. The design of modern running time anemometers with delay time measurements were developed by Hanafusa et al. (1982) and Coppin and Taylor (1983) and it has been the conventional approach to measure turbulent fluxes for 30 years in different environments (Aubinet et al., 2012; Baldocchi et al., 1988; Grimmond, 2006; Lee et al., 2004). The modern EC observation setup includes commonly an ultrasonic anemometer, for measuring the three dimensional wind and sonic temperature and an infrared gas analyser for measuring gas concentrations.

The observational challenge in the EC technique particularly in urban areas is to expose the instruments appropriately, so that the recorded data provides useful and representative information of the study area. Thus, the EC observations should be made in the inertial sublayer (Grimmond et al., 2002; Grimmond, 2006; Oke, 2008) where the fluxes are assumed to be approximately constant with height (Aubinet et al., 2012). Hence the measurements are assumed to be representative of the underlying urban ecosystem and free from the microclimatic effects of individual urban facets. In order to make measurements in inertial sublayer in urban areas, the instruments should be placed at least to 1.5 times the height of main roughness elements (buildings and trees) (Grimmond and Oke, 1999; Oke, 2008; Raupach et al., 1991; Rotach, 1999). In addition, the instruments should be placed in narrow lattice towers to assure that the exposure of the instruments is free from flow distortion (Roth, 2000). However, choosing an ideal location for EC measurements in urban areas is hardly possible due to the heterogeneity of urban surfaces. In addition, the limitations due to logistical and safety restrictions and the need to have public acceptance, measurements often have to be made from existing towers (e.g. telecommunication towers) or on top of buildings (Ao et al., 2016; Brümmer et al., 2012; Keogh et al., 2012; Liu et al., 2012; Nordbo et al., 2013; Wood et al., 2010), which are restricted in height and are bulkier than narrow lattice masts which would minimize the effect of the structure itself on the measurements. Thus the EC measurements at urban areas are not necessarily made completely free of the impact of roughness elements even if the measurement height would be at a sufficient height above the surrounding roughness elements.

Despite the challenges in EC measurements due to complexity and heterogeneity of urban surfaces and logistical limitations, useful observations can be obtained, when proper consideration of the placement of instruments have been taken (Oke, 2008).

2.3 Numerical modelling

Examining urban climate with observations alone is limited by the technological limitations. In addition, some parts of the urban atmosphere are unreachable by observations due to practical restrictions and predictions of the effects of future urban development scenarios can not be made with measurements. Many urban effects are subtle in nature and interactions are complex between the urban drivers. Therefore numerical models are fundamental tools in analysing these effects by allowing real world complexity to be simplified and by isolating certain processes of interest. Thus properly evaluated numerical models can be important tools in urban planning and design.

Numerical modelling in general simulates real world phenomena using a set of equations that link meteorological properties to land surface processes (e.g. energy and water balances). Depending on the type of model and its application, some of the equations governing the land-surface interaction can be simplified or even omitted. For example, urban models commonly focus on either airflow or surface energy fluxes, where the other is handled with parametrisation rather than to fully model their interaction. This ability to isolate certain processes is one of the defining attributes of numerical models.

A variety of urban land surface models with varying complexity have been developed to understand the urban land-surface interaction (Grimmond et al., 2010b, 2011). From highly abstract models used only to guide research, to those used to predict and analyse real world phenomena and simulate the urban climate under different urban development scenarios. One of the first models to study urban energy balance was introduced by Myrup (1969), that represented the urban environment as an extensive homogeneous surface. After that many urban land surface models have been developed, such as simple single-layer urban canopy model (Kusaka et al., 2001), Building Effect Parameterization (BEP; Martilli et al., 2002), multilayer urban canopy model (Kondo et al., 2005) and Community Land Model–Urban (CLM-Urban; Oleson et al., 2008). Typically these models are designed to represent the urban energy balance of idealized urban canopy consisted from various urban facets, but originally without the effect of vegetation. In central downtown locations of major cities a model design without an inclusion of vegetation might be a reasonable simplification, but in many suburban areas vegetation has a significant influence on urban latent heat flux (Best and Grimmond, 2016; Grimmond and Oke, 1986; Demuzere et al., 2014; Mitchell et al., 2001b, 2003; Oke et al., 2017; Templeton et al., 2018, **Paper III**). The first international urban model comparison experiment concludes also that the models with a representation of vegetation performed much better in simulating latent and sensible heat fluxes than the models neglecting it (Best and Grimmond, 2015, 2016; Grimmond et al., 2011) even though urban land surface models tend to underestimate vegetative evaporation (Grimmond et al., 2010b, 2011). Therefore models which have the description of vegetation, are important in understanding urban energy and water balances. Thus the newer models (e.g. Surface Urban Energy and Water Balance Scheme (SUEWS; Järvi et al., 2011, 2014) and SURFEX (Masson et al., 2013)) have the description of the vegetation and the other above mentioned models have also included vegetation afterwards.

Also a variety of urban hydrological models have been developed to examine the water balance and flow within the urban areas (Peña-Guzmán et al., 2017; Obropta and Kardos, 2007). One of the most used ones include EPANET (Rossman, 1993), Aquacycle (Mitchell et al., 2001a) and Storm Water Management Model (SWMM; Rossman, 2015). However, these models are focusing mostly on water distribution in cities and design of pipe networks. For example, the EPANET is commonly used to simulate the potable water quality and its transport in the distribution systems (e.g. Kurek and Ostfeld, 2013; Shang et al., 2008; Tabesh et al., 2009). The Aquacycle has been used especially in studies of reuse schemes of storm water and waste water in cities (e.g. Lee et al., 2010; Sharma et al., 2008; Zhang et al., 2009), since in the model storm water and waste water can be stored separately and used in the source of supply in the non-potable water applications. The SWMM has been used mainly in studies related to design of pipe networks and dynamic flood routing (e.g. Jia et al., 2012; Meierdiercks et al., 2010; Qin et al., 2013), since it includes schemes for flow depth of water in each pipe of the study area and routing of above ground runoff along with pumps, regulators, pipes and channels. However, the description of evaporation is often insufficient in these models. Thus, the modelling community of the above mentioned hydrological models, where the applications of the model results are more directly connected to urban engineering, also benefit from the results of this thesis which brings improved understanding of the urban effects on the hydrological cycle.

SUEWS model (Järvi et al., 2011, 2014, see Section 3.2) is used in this thesis (**Papers II, III and IV**). The advantages of SUEWS are its ability to model both energy and water balances, easy usability and forcing with commonly available meteorological variables. This allows the usage of the model also when extensive amount of data for forcing are not available, as for the studies of the past conditions (**Paper III**) or in the areas where the available data are scarce (**Paper IV**). SUEWS has also been shown to perform well against sensible and latent heat flux, runoff, soil moisture and snow observations in varying climate conditions in different cities (e.g. Alexander et al., 2015; Demuzere et al., 2017; Järvi et al., 2011, 2014, 2017; Karsisto et al., 2016; Ward et al., 2016, 2018).

Figure 2: Map showing the locations of the study areas.

3 Hydrological modelling

3.1 Study sites and measurements

The study areas cover a wide range of urban structures in different climates around the globe (Figure 2). The study areas in Helsinki, London and Beijing are within a dense city centre locations whereas the Vancouver study sites, Oakridge and Sunset, are located at suburban residential areas. The site characteristics are ranging from 53% of impervious surfaces with 47% of vegetation and population density of 28 inh ha^{-1} in Oakridge to 81% of impervious surfaces with only 5% of vegetation and population density of 310 inh ha^{-1} in London (Figure 3, Table 1). All of the study areas have meteorological observation stations including eddy covariance towers allowing evaluation of the model results and reanalysis data (Table 2). In addition, Helsinki study site has two identical EC setups which allow analysis of the uncertainties in EC observations when comparing the results.

Table 1: Study site characteristics.

	Helsinki[a]	Vancouver[b]		London[c]	Beijing[d]
		Oakridge	Sunset		
Latitude (WGS84)	60°10'N	49°13'N	49°13'N	51°30'N	39°58'N
Longitude (WGS84)	24°56'E	123°08'W	123°05'W	0°7'W	116°22'E
Time zone	UTC+2	UTC-8	UTC-8	UTC	UTC+8
Study height (m agl)	60	28	28	49	47
Base elevation (m asl)	15.2	85	82	12	60
Study area (ha)	196	22.5	14.9	78.5	314.2
Population density (inh ha^{-1})	81	26	82	310	142
Fraction of buildings	0.37	0.24	0.29	0.38	0.24
Fraction of paved surfaces	0.40	0.29	0.37	0.43	0.46
Fraction of trees/shrubs	0.15	0.14	0.07	0.02	0.13
Fraction of grass	0.07	0.33	0.27	0.03	0.16
Fraction of water	0.01	0.00	0.00	0.14	0.01
Mean building height (m)	24.0	6.0	5.9	22.0	19.1
Mean tree height (m)	8.3	8.0	7.1	13.1	8.0

[a]From Nordbo et al. (2015)

[b]from **Paper III** for 2009

[c]from **Paper II**

[d]from **Paper IV**

Table 2: Instrumentation at the study sites.

Study site	Instrument	Model	Manufacturer	Reference
Helsinki	3D sonic anemometer	USA-1	*Metek GmbH*	Wood et al. (2013)
	Infrared gas analyser	LI-7200	*LI-COR Biosciences*	
Oakridge	Rain gauge	Tipping bucket	*R.M. Young Company*	Grimmond and Oke (1986)
	Radiometer	PSP	*The Eppley Laboratory*	
	Air temperature / relative humidity	HMP T/RH sensor	*Vaisala*	
Sunset	3D sonic anemometer	CSAT-3	*Campbell Scientific*	Christen et al. (2011)
	Infrared gas analyser	LI-7500	*LI-COR Biosciences*	
	Radiometer	CNR1	*Kipp & Zonen*	
	Rain gauge	Tipping bucket	*R.M. Young Company*	
	Air temperature / relative humidity	HMP T/RH sensor	*Vaisala*	
London	3D sonic anemometer	CSAT-3	*Campbell Scientific*	Kotthaus and Grimmond (2014a,b)
	Infrared gas analyser	LI-7500	*LI-COR Biosciences*	
	Radiometer	CNR1	*Kipp & Zonen*	
	Weather station	WXT510	*Vaisala*	
	Rain gauge	ARG100	*Campbell Scientific*	
Beijing	3D sonic anemometer	CSAT-3	*Campbell Scientific*	Liu et al. (2012)
	Infrared gas analyser	LI-7500	*LI-COR Biosciences*	
	Radiometer	CNR1	*Kipp & Zonen*	
	Weather station	Developed by the IAP*		
	Aerosol optical depth	CE-318	*Cimel Electronique*	Che et al. (2009)

*Institute of Atmospheric Physics, Chinese Academy of Sciences, Beijing

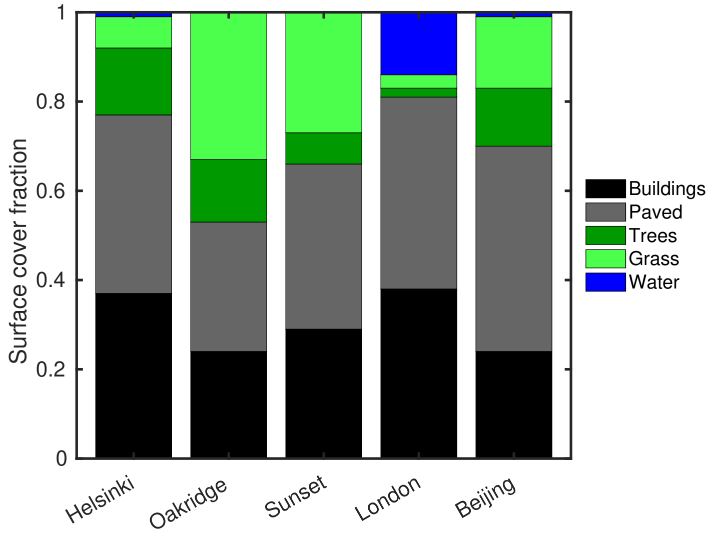

Figure 3: Surface characteristics of the study areas. Data from Table 1.

3.1.1 Helsinki

Helsinki experiences cold temperate climate with significant influence of the sea (Kersalo and Pirinen, 2009). The precipitation is generally evenly distributed throughout the year with high monthly precipitation totals during summer and late fall (Kersalo and Pirinen, 2009).

The study site is in central Helsinki and the measurements are located next to masonry on top of the Hotel Torni building. The surrounding area is fairly homogeneous with mean building height of 24 m. The centre of Helsinki is located at a peninsula, but previous analysis have shown that the flux footprint lies above the city and not the sea (Auvinen et al., 2017; Kurppa et al., 2015). Two identical instrument setups (Table 2) were installed on the opposite sides of a bulky masonry on top of the Hotel Torni building tower with a distance of 10 m apart from each other, which indicates that both systems are measuring virtually the same source area. This allows the analysis of uncertainties caused by a single urban EC measurement by comparing the measurements of the two identical setups.

3.1.2 Vancouver

Vancouver experiences maritime temperate climate (Oke and Hay, 1994). The winter time precipitation totals are approximately four times the summer precipitation totals and therefore there is a substantial amount of garden irrigation in Vancouver during summer months (Grimmond and Oke, 1986).

The study sites in Vancouver are two suburban areas (Oakridge and Sunset) located approximately 3 km apart in a fairly flat terrain. Both areas have 1–2 storey single-family dwellings with mean building height of 6.0 and 5.9 m, respectively, but have different land cover fractions and lot sizes. The more prosperous (e.g. Statistics Canada, 1988) Oakridge area has bigger lots and houses and well maintained gardens with more automatic irrigation systems than Sunset area.

3.1.3 London

London experiences maritime temperate climate, which is occasionally influenced by continental weather that brings cold spells in winter and hot and humid weather in the summer (Met Office, 2016). The precipitation in London is generally evenly distributed throughout the year, with significant amounts of convective rainfall in the summer (Met Office, 2015).

The London study site is located in central London at the rooftop of King's College. The study area is the central business district of Westminster, which has an extensive amount of impervious surfaces (81%), mean building height of 22 m and insignificant irrigation. The area has a large daytime population and high volume of traffic (Greater London Authority, 2015), which makes anthropogenic heat fluxes an important part of the energy balance (Ward and Grimmond, 2017; Ward et al., 2018).

3.1.4 Beijing

Beijing experiences monsoon driven continental climate (Domrös and Peng, 1988) and suffers from severe atmospheric pollution (Kulmala, 2015). The winter time in Beijing is very dry and most of the precipitation comes during the summer monsoon season (Beijing Municipal Bureau of Statistics, 2016).

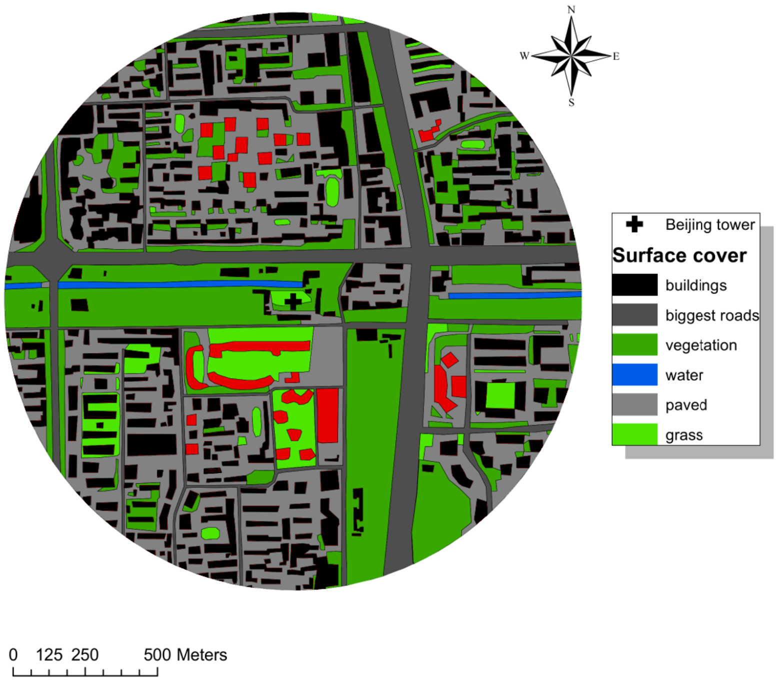

Figure 4: Surface cover of the study area around the 325 m IAP tower. Tall buildings (over 50 m) are shown in red color. Modified after Murto (2017).

The study site is around the 325 m high Institute of Atmospheric Physics (IAP) meteorological tower in the northwest part of Beijing. At the time the tower was built the surroundings were lower built up area and rural croplands. As a result of rapid urban sprawl, the tower is nowadays located at a densely built urban area. The measurements are made at the 47 m level which from some wind directions (mainly from southwest and northwest) is in the roughness sublayer due to high-rise buildings (Figure 4; Miao et al., 2012) and therefore the EC data from these wind directions (314–3°, 40–45°, 112–128°, 160–243°) are filtered out (34% of the data). From other wind directions the surroundings are fairly homogeneous with mean building height of 19.1 m (Miao et al., 2012).

3.2 Model description

The hydrological modelling in this thesis is conducted using the Surface Urban Energy and Water Balance Scheme (SUEWS; Järvi et al., 2011, 2014). SUEWS is an urban land surface model that simulates the surface energy and water balances at the local scale (neighbourhood scale), which corresponds to the spatial scale used in planning and design related to land use and infrastructure in cities (Kellett et al., 2013). SUEWS has seven parallel hydrologically connected surface types (buildings, paved surfaces, evergreen trees/shrubs, deciduous tree/shrubs, grass and water; Figure 5). Underneath each layer there is a single soil layer excluding the water surface. The model is run with 5 min time step to allow rapid response to the changes in the water balance. The evaporation is calculated for each surface using the Penman-Monteith equation (Monteith, 1965; Penman, 1948) modified for urban environments (Grimmond and Oke, 1991) and runoff from a running water balance (Grimmond and Oke, 1991; Järvi et al., 2011). The fluxes calculated for an individual time step are a function of the proportion of the component surface types in the area.

SUEWS has several submodels (e.g. for net all-wave radiation, irrigation and anthropogenic heat flux) designed to minimize the needed input data. The irrigation submodel is important especially for **Paper III**, where the impact of various irrigation scenarios on urban hydrological cycle are explored. SUEWS can run without extensive computing power forced with commonly available meteorological data (wind speed (U), relative humidity (RH), air temperature (T_a), pressure (p), precipitation (P) and incoming solar radiation ($K\downarrow$)) and information about the surface characteristics of the modelled area, including plan area fractions, tree and building heights and population density.

SUEWS performance and sensitivity to input variables and model parametrisation has been extensively evaluated in the earlier studies for multiple variables in different climates (e.g. Alexander et al., 2015; Demuzere et al., 2017; Järvi et al., 2011, 2014, 2017; Karsisto et al., 2016; Ward et al., 2016, 2018) and the model has been found to perform well in modelling sensible and latent heat fluxes in comparison with other urban land surface models (Grimmond et al., 2010b, 2011). Additional evaluation of SUEWS performance and sensitivity testing are made in this thesis (**Papers II, III and IV**).

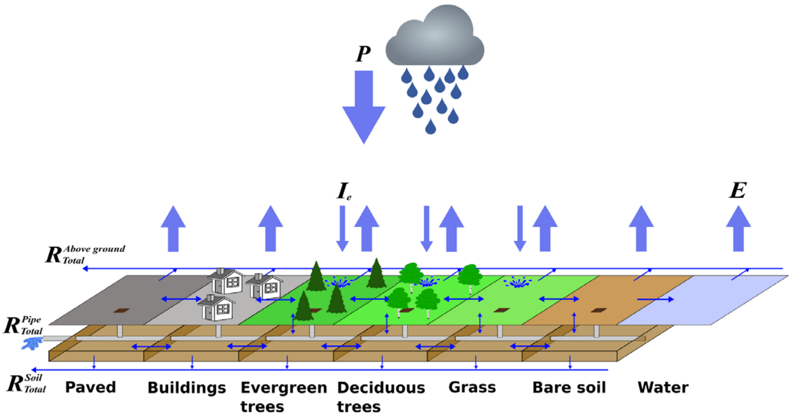

Figure 5: The surface types and water flows in the SUEWS model. P is precipitation, E is evaporation, I_e is irrigation, R_{Total}^{Soil} is total soil runoff, R_{Total}^{Pipe} is total pipe runoff, $R_{Total}^{Above\ ground}$ is total above ground runoff. Total surface runoff is a sum of R_{Total}^{Pipe} and $R_{Total}^{Above\ ground}$. Modified after Ward et al. (2017).

3.3 Reanalysis forcing data

The reanalysis data used and evaluated in this thesis (**Papers II, III and IV**) are the WATCH Forcing Data WFD (1919–1979; Weedon et al., 2011) and WFDEI (1980–2013; Weedon et al., 2014). These datasets have been derived specifically for the hydrological modelling from ERA-40 (Uppala et al., 2005) and ERA-Interim (Dee et al., 2011) reanalysis products via sequential interpolation to half-degree spatial resolution and 3 to 6 h temporal resolution. For the precipitation, WATCH data provides two alternative bias correction methods: the Climatic Research Unit Time Series (CRU; Harris et al., 2014) and the Global Precipitation Climatology Centre (GPCC; Schneider et al., 2013). The GPCCv4/v5/v6 bias corrections are used in this thesis since the number of stations used for the bias correction is much higher (Weedon et al., 2011) and it has shown to perform better in hydrological modelling (Essou et al., 2016).

In order to have realistic forcing data for local scale urban hydrological modelling from WATCH data, a few corrections are needed due to coarse spatial resolution (**Papers II and IV**) and the lack of description of urban environments in IFS-model used in production of ERA-Interim reanalysis. First, the air temperature and pressure are adjusted to simulation height using environmental lapse rate ($\Gamma = -6.5$ K km^{-1}) and the hypsometric equation (Weedon et al., 2010). Second, in order to remove bias between the WATCH precipitation representing 0.5°grid and local city precipitation rates, the reanalysis precipitation is corrected using bias correction with quantile mapping (BCQM, see Section 3.6) for the daily totals (**Paper II**). Third, the incoming solar radiation is corrected to account for the additional effect of local air pollution (**Paper IV**) using correction factors obtained from the observations of incoming solar radiation and aerosol optical depth.

3.4 Surface characteristics

In order to capture the effect of densification on local urban hydrological cycle (**Paper III**), the detailed surface cover fractions need to be determined at the scale of individual lots. Even the latest algorithms are not able to determine the cover fractions from older aerial photographs with poor quality in sufficient detail (Tokarczyk et al., 2015) and therefore the fractions have to be analysed manually for **Paper III** (Figure 6).

Other surface characteristic needed by SUEWS (population density for calculation of Q_F, building and tree height for calculation of aerodynamic roughness length and zero displacement height) can be obtained from the census data (Vancouver, Beijing) and the lidar scans of the study area (Helsinki, London). If this data is not available for the analysed period, the characteristics have to be derived indirectly. In **Paper III** the tree height is determined using urban tree growth models described in McPherson et al. (2016a) with empirical equations from McPherson et al. (2016b) due to lack of historical data.

3.5 Experimental setup

In **Paper I** EC observations using two identical measurement systems are performed in central Helsinki between July 2013–September 2015. The raw EC data are sampled with a 10 Hz frequency, from which the 30 min flux values are calculated using commonly accepted methods (Nordbo et al., 2012).

In **Paper II** a full year is simulated with SUEWS (V2016a) in London and Vancouver Sunset (2012 and 2009, respectively) for the EC footprint area. Vancouver Oakridge is

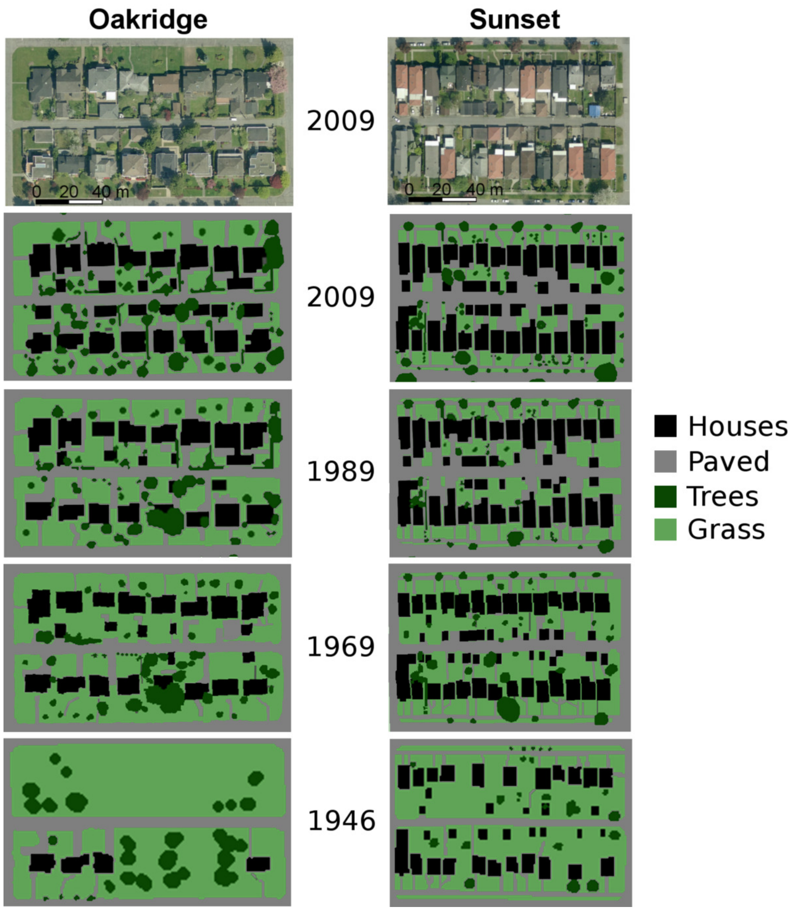

Figure 6: Exmples of surface cover fractions determined manually from aerial photographs for Oakridge and Sunset neighbourhoods in Vancouver for one example block of the study areas (upper panels) for different years. Adapted from **Paper III**.

simulated for 22 January 1982–21 January 1983 for the water monitoring area (Grimmond and Oke, 1986). Simulations are made using hourly, locally measured data and WATCH WFDEI reanalysis data. The WFDEI data are interpolated from 3 h to 1 h resolution and further to 5 min time step of SUEWS within the model. The WFDEI precipitation data are bias corrected using BCQM method.

In **Paper III** SUEWS is run between 1919–2010 in Vancouver Oakridge and Sunset using the first year as a spin-up leaving years 1920–2010 for the analyses. The simulations are made using WATCH WFD (1919–1979) and WFDEI (1980–2010) reanalysis data. The 3 to 6 h resolution WATCH data are first interpolated to 1 h resolution, which is the recommended temporal resolution of the forcing data for SUEWS V2016a. The forcing data are further interpolated to 5 min time step of SUEWS within the model. The WFDEI precipitation data are bias corrected using BCQM method.

In **Paper IV** the simulations are made between 2000–2013 in Beijing. Spin-up for one year leaves 2001–2013 for the analyses. The WFDEI reanalysis data are interpolated from 3 h temporal resolution straight to 5 min time step of SUEWS (V2017b) within the model. The WFDEI precipitation data are bias corrected using BCQM method and incoming solar radiation data are corrected using regression coefficients determined from observations.

3.6 Statistical methods

Statistical analysis in this thesis are performed using commonly used methods. The correlations among different variables are analysed using Pearson's correlation coefficient (R), root mean square error (RMSE) and RMSE normalised with standard deviation of observations (nRMSE), mean bias error (MBE), MBE normalised with mean of observations (nMBE), mean absolute error (MAE) and MAE normalised with mean of observations (nMAE). A Lowess smoothing (Cleveland, 1979, 1981) is applied to a scatter of incoming solar radiation and AOD observations in **Paper IV** prior to calculating the regression coefficients.

The quality of EC data in **Paper I** is evaluated using stationarity (FS), skewness (SK) and kurtosis (K). FS provides information about the stationarity of the flux measurements and SK and K provide information about the form of the probability function of the measured concentration, temperature or wind speed (Vickers and Mahrt, 1997).

The relative random error (RRE) of the vertical flux of scalar is calculated following the method in Lenschow et al. (1994). The power and cospectra of fluxes are calculated according to Stull (1988).

The precipitation is corrected in **Papers II, III and IV** using bias correction with quantile mapping (BCQM) following the methods in Räty et al. (2014) and Räisänen and Räty (2013). This method is widely used in bias correction of temperature and precipitation data for climate projections and hydrological models (e.g. Dosio and Paruolo, 2011; Piani et al., 2010; Sun et al., 2011).

The long-term changes of daily runoff events in **Paper III** are evaluated using occurrence frequency analysis calculated with empirical Weibull (1939) formula, which is a method recommended by World Meteorological Organization (2011) for hydrological return period analysis. The long-term trend analysis are made using the Mann-Kendall trend test (Kendall, 1975; Mann, 1945), which is one of the most widely used methods to detect trends in hydrological time series (e.g. Hirsch et al., 1982; Lins and Slack, 1999; Pechlivanidis et al., 2017).

The performance of the model runs and WFDEI variables in **Paper IV** are evaluated using a Taylor (2001) diagram.

In addition to the comparison of medians of the results from **Paper IV**, a two-tailed Student's t-test is applied to examine the statistical significance of the results compared.

4 Key results

4.1 Uncertainties in eddy covariance measurements

The filtering of the data from the flow distortion areas of the two identical instrument setups (EC1 and EC2), due to the masonry of the building, removes 27% of the EC1 data and 38% of the EC2 data. The emissions of greenhouse gases in cities are commonly calculated from emission inventories on an annual level and the removal of the EC data can cause systematic errors in the annual cumulative fluxes. Therefore it is also important to understand the biases of annual cumulative fluxes in the observations. For latent and sensible heat fluxes this is not as important, but in order to eliminate the random error, the biases in these fluxes are analysed also on an annual level.

For the calculation of annual cumulative latent and sensible heat fluxes, EC1 and EC2 are both gap-filled with their own median cycle using a 3 month period around the month being gap-filled with a separation to workdays and weekends (and holidays). Also combination of EC1 and EC2 is used by taking the data in the flow distortion areas from the undisturbed instrument setup and for the other directions the mean of the two systems is calculated. To estimate the bias caused by the single point measurement, the data of each of the setups are compared to annual cumulative fluxes combined from both of the setups. Even though the measurement location of the two EC systems is not ideal and it leads to rather large removal of the data due to the flow distortion, the possible bias caused by the single point measurement is an underestimation of 8% for the latent heat flux (5% for Q_H) when compared to flux obtained from combination of the two systems. This indicates that single point EC observations can produce reasonable estimations of latent and sensible heat fluxes even in complex urban environments with non-ideal instrument location with wide flow distortion area when the surrounding urban surface is relatively homogeneous.

Even though the filtering of the EC data from the Beijing IAP tower removed 34% of the data due to the flow distortion from certain wind directions (Section 3.1.4), based on the results in **Paper I**, the remaining data can be assumed to be representative of the conditions on the remaining source area with fairly homogeneous surface characteristics.

The random uncertainties of flux measurements have been determined in past studies above vegetated ecosystems using the two-tower approach (Hollinger and Richardson,

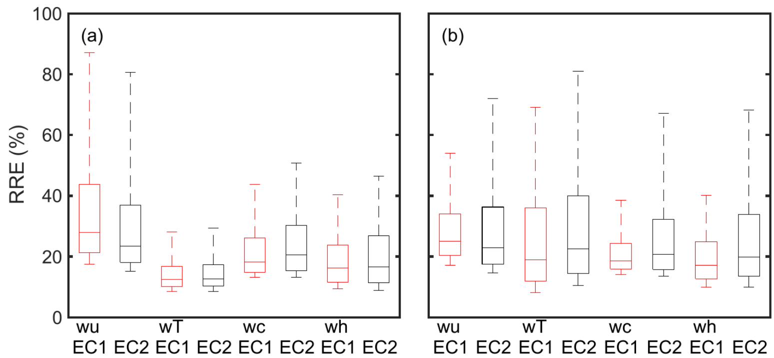

Figure 7: Relative random error (RRE) for (a) daytime (solar elevation angle >0°) and (b) night-time (solar elevation angle ≤0°) momentum (wu), heat (wT), CO_2 (wc) and water vapour (wh) covariances from the two systems EC1 and EC2 outside the flow distortion sectors. Whiskers and boxes represent the 10th, 25th, 50th, 75th and 90th percentiles. Adapted from **Paper I**.

2005; Kessomkiat et al., 2013). The assumption in the method is that the two time series should be independent from each other, which is not true in this case since both of the systems are measuring the same footprint. However, the relative random error (RRE) can still be calculated independently for the two systems to get an understanding of the random uncertainties of the EC measurements in this case. The random uncertainty in latent heat flux is approximately 18% (13% in Q_H) with night-time uncertainties being slightly larger than daytime (Figure 7). In addition, the coefficient of determination (R^2) between the two systems is assumed to be also a measure of the random uncertainty. Theoretically when RRE is high R^2 should be low. The R^2 of latent heat flux is found to be 0.79 in daytime and 0.66 in night-time. It is expected result that the random uncertainties are larger during the night-time when the fluxes are smaller. The random uncertainties found at this study in dense urban environment are slightly larger but in the same order of magnitude as observed earlier above vegetated ecosystems (Hollinger and Richardson, 2005; Kessomkiat et al., 2013; Peltola et al., 2015; Post et al., 2015).

4.2 Evaluation and corrections of the reanalysis data

Evaluation of WATCH WFDEI reanalysis data (Weedon et al., 2014) is performed in **Papers II and IV**. The effects of reanalysis input data to biases of SUEWS results are evaluated using sensitivity tests of individual reanalysis variables in Vancouver and London (**Paper II**). SUEWS is run with observed forcing data while each variable is systematically replaced with the WFDEI equivalent. The modelled annual cumulative evaporation and runoff using the different combinations of forcing data are then compared to the control run (observed forcing data for all input variables). The evaluations in **Paper II** are made on an annual level, since the long-term analyses in **Paper III** focus mainly on annual values.

The model bias increases the most when changing uncorrected WFDEI precipitation data in otherwise observed forcing data, while RH being the second most important. The uncertainty caused by the uncorrected WFDEI precipitation to annual cumulative evaporation is 14–26% and runoff 7–39% when compared to the control run. The biases induced by WFDEI RH when compared to the control run are 3–9% and 1–2% for evaporation and runoff, respectively. Other WFDEI variables (U, T_a, $K\downarrow$ and p) have only minor effect on modelled evaporation and runoff in rather clean environments of Vancouver and London, with bias up to 4% when compared to the control run.

Based on the results of **Paper II**, precipitation is the most crucial input variable to correct in order to have realistic model results using SUEWS forced with WFDEI reanalysis data. Therefore bias correction using quantile mapping (BCQM, see Section 3.6) is applied to WFDEI precipitation to correct the biases in the reanalysis data in Vancouver, London and Beijing (**Papers II, III and IV**). In Vancouver the daily cumulative WFDEI precipitation overestimates the precipitation totals in all of the intensity bins, while in London and Beijing the daily totals are slightly overestimated only with smaller daily totals and underestimated with higher daily totals (Figures 8 and 9). After the BCQM correction applied, the WFDEI precipitation follows the observations rather well except in Oakridge which still has substantial biases: 21.7%, 3.9%, 1.6% and -5.9% deviation from the observed annual cumulative precipitation in Oakridge, Sunset, London and Beijing, respectively. The BCQM correction decreases the biases in model results of evaporation for 4–15% and runoff for 0–20%, resulting to overestimation of 10–11% in evaporation and biases from -7 to +19% in runoff, when comparing to the control run in **Paper II**.

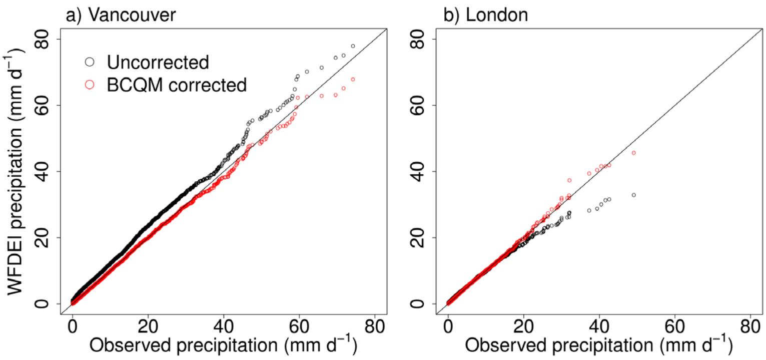

Figure 8: Quantile-quantile plots for uncorrected WFDEI daily precipitation and BCQM corrected daily precipitation versus observed precipitation (1990–2008 in a) Vancouver and 1979–2012 in b) London). Both Vancouver study sites (Oakridge and Sunset) use precipitation data from the same WFDEI grid. Adapted from **Paper II**.

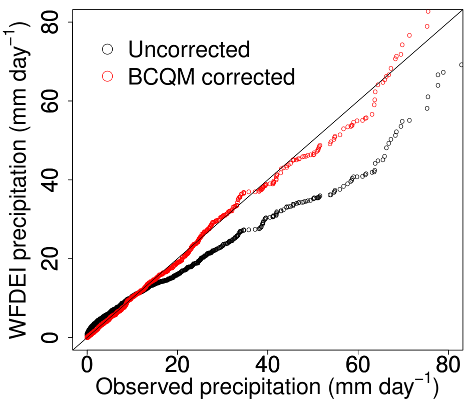

Figure 9: Quantile-quantile plots for uncorrected WFDEI daily precipitation and BCQM corrected daily precipitation versus observed precipitation (1980–2012) in Beijing. Adapted from **Paper IV**.

The most important input variables for hydrological modelling with SUEWS have been identified in earlier studies (Alexander et al., 2015; Ward and Grimmond, 2017, **Paper II**). In **Paper IV** the same variables of WFDEI data are evaluated in highly polluted Beijing. The overestimation of WFDEI $K\downarrow$ increases with the level of pollution when compared to observations (nMBE: -0.01, 0.00, 0.08, 0.28; fairly clean (AOD<0.203), low pollution (0.203–0.438), polluted (0.438–1) and extremely polluted air (>1), respectively), which indicates that the attenuating effect of haze on incoming solar radiation is not properly accounted for in the WFDEI reanalysis data. This is presumably related to the large grid size of the WFDEI data and the insufficient description of urban aerosol processes (e.g. neglecting urban secondary nucleation). Therefore WFDEI $K\downarrow$ is corrected using observations between 2006–2009 from the 325 m IAP measurement tower (Table 2) separately for thermal summer months (Apr–Sept) and winter months (Oct–Mar) due to slightly different behaviour. Regression coefficients are calculated for observed $K\downarrow$ normalised with clear sky radiation ($I_{SC} \times \cos\theta_z$, where I_{SC} is solar constant (1367 W m^{-2}) and θ_z is the solar zenith angle) versus AOD after Lowess smoothing applied to scatter. This correction improves substantially the WFDEI $K\downarrow$ making the different air quality levels equally good corresponding well with the observed behaviour (nMBE: -0.01, 0.00, -0.03, -0.03 from clean to extremely polluted conditions)(Figure 10). The other evaluated variables (RH and T_{air}) correlate well with the observations (R>0.68) and the nMBE is rather good (<0.26) and the performance is equally good with different pollution levels (Figure 10), so there is no need for bias correction. However, there are still substantial biases in P even after the BCQM correction, since the bias correction does not work as well for the high pollution levels due to low amount of precipitation during the more polluted conditions

Earlier sensitivity tests show that the model sensitivity to input variables depends on the type of urban area in focus. When the study site is in a suburban area (LCZ 6; Stewart and Oke, 2012), the model is more sensitive to the accuracy of the meteorological input data than for the description of land cover (Alexander et al., 2015). However, for dense city centre areas (LCZ 2) the land cover description is more crucial and the model is rather insensitive to the quality of the meteorological input data (Alexander et al., 2015).

The reanalysis datasets are openly available with global coverage and therefore provide accessible and easy to use input data needed for hydrological modelling. Thus, the improved understanding of the uncertainties in reanalysis data and the downscaling

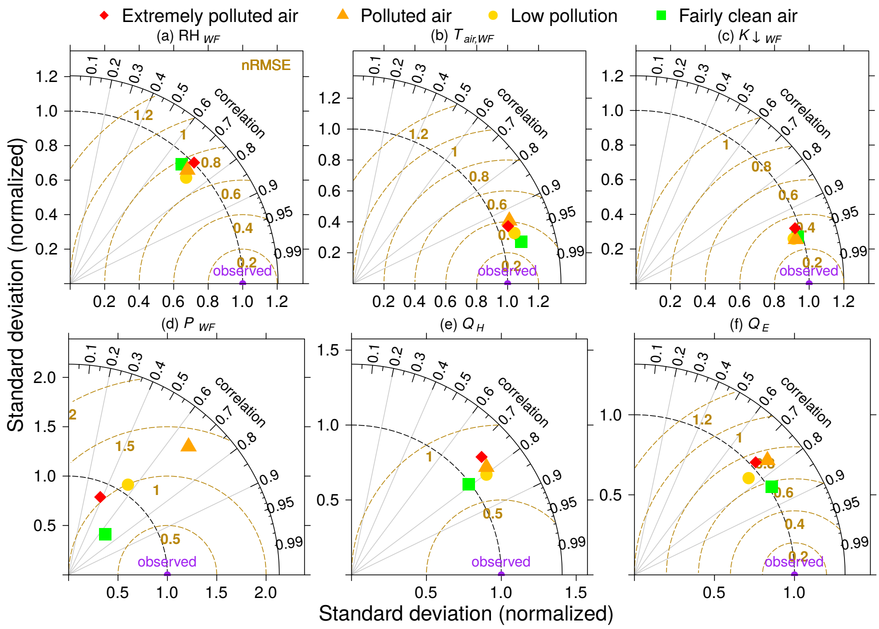

Figure 10: Taylor diagram (Taylor, 2001) for hourly (a) relative humidity (RH_{WF}), (b) air temperature ($T_{air,WF}$), (c) incoming solar radiation ($K{\downarrow}_{WF}$ and daily (d) precipitation (P_{WF}) with corrected WFDEI data assessed with IAP observations stratified by air quality, and hourly modelled (e) sensible heat flux (Q_H) and (f) latent heat flux (Q_E) against eddy covariance IAP observations from 47 m height for 2006–2009. The pollution levels are: extremely polluted (AOD>1), polluted (0.438–1), low pollution (0.203–0.438) and fairly clean air (<0.203). The radial axis is normalised standard deviation, angular axis is correlation coefficient and brown dashed lines indicate normalised root-mean square error. See Section 3.6 for statistics explanation. Adapted from **Paper IV**.

for the local scale in urban areas will benefit meteorological modelling in urban areas and engineering modellers. The methods used in this thesis to evaluate and downscale reanalysis data can presumably be utilized globally in varying urban environments.

4.3 Evaluation of SUEWS

The evaluations of SUEWS in modelling latent heat flux against eddy covariance observations are performed in Vancouver, London and Beijing (**Papers II and IV**). SUEWS forced with corrected WFDEI reanalysis data (see Section 3.3) is underestimating the annual cumulative evaporation by 15% in Sunset for 1982 and overestimating by 31% in London for 2012. The underestimation in Vancouver Sunset is an expected result since urban land surface models tend to underestimate vegetative evaporation (Grimmond et al., 2010b, 2011). Thus, the model results with observed forcing data also underestimate the evaporation by 18% in Sunset. Therefore the underestimation in Sunset is expected to be linked to the description of evaporation in SUEWS rather than biases in WFDEI forcing data. However, the overestimation in London is expected to be due to the proximity of River Thames to the EC measurements. The surface cover fractions in SUEWS are calculated for the source area of EC observations leading to 14% of open water, which causes large evaporation rates. However, the river itself does not affect the EC observations as much partly because potential internal boundary layers forming over the water surface might not develop to the height of the EC tower (Kotthaus and Grimmond, 2014b). The overestimation in London is 23% when using observed forcing data.

SUEWS model performance is relatively independent of air quality since the effects are included in the input variables $K\downarrow, T_a$ and RH. As the incoming longwave radiation ($L\downarrow$) emitted by the sky is calculated in SUEWS from T_a and RH, which have positive correlation with the increasing level of pollution in Beijing (e.g. Cai et al., 2017; Chen and Wang, 2015; Wu et al., 2017, **Paper IV**), the positive correlation of $L\downarrow$ and air quality is successfully reproduced by SUEWS. The incoming longwave radiation is not evaluated due to lack of observations, but the increasing $L\downarrow$ with the level of pollution follows rather well the assumption reported in earlier studies that the aerosols emit more longwave radiation with increasing amount of air pollution (e.g. Cao et al., 2016; Jacobson, 1998). Therefore, the model performance is reasonably good when comparing to IAP EC observations and does not decrease substantially with increasing

AOD (Figure 10) making the different pollution levels generally comparable with each other (R>0.73, nRMSE: 0.58 to 0.81 from clean to extremely polluted conditions).

The SUEWS model performance in Vancouver, London and Beijing forced with the corrected WFDEI reanalysis data is similar to SUEWS performances in other studies in Vancouver, Los Angeles, London and Swindon using observed forcing data (e.g. Järvi et al., 2011; Ward et al., 2016). In addition, other local scale urban models used previously in Beijing have had similar performance in modelling latent and sensible heat fluxes (e.g. Liang et al., 2018). Even though surface fluxes describe only certain parts of land surface models, good correspondence between model results and observations of sensible and latent heat fluxes indicate smaller uncertainties also in other components of water and energy balances which are commonly much harder to evaluate. Therefore model results of SUEWS forced with corrected WFDEI reanalysis data can be used relatively reliably in all of the study sites in this thesis, even in the highly polluted Beijing.

4.4 Factors affecting urban hydrological cycle

As the model performs well in all of the study sites, it allows detailed analyses of the effects of urban development on the local scale urban hydrological cycle. To understand the proportional effects of urban development processes (urbanisation, densification, increased irrigation, worsening air quality) and to identify the most important factors, different processes are examined also individually (**Papers III and IV**).

Garden irrigation has a dominant impact on the urban hydrological cycle over the urbanization and densification (Figure 11; **Paper III**) at the two suburban study sites, Oakridge and Sunset, in Vancouver (Section 3.1.2). This is expected as the irrigation accounts up to 56% of the water input annually and up to 89% during the irrigation period (May–August), based on the model results using realistic irrigation scheme (irrigation started in 1951) and taking into account lawn watering restrictions from 1992 onwards in Vancouver. Annual cumulative surface runoff is linearly dependent on the amount of irrigation. When irrigation is doubled, runoff increases 38% and 37% in Oakridge and Sunset, respectively (Figure 12). However, evaporation increases rapidly with smaller annual irrigation totals to a threshold value of 300 mm year^{-1} which after it is energy limited and the excess water is going to runoff and is not usable by the garden and its plants. Similar thresholds of evaporation have been

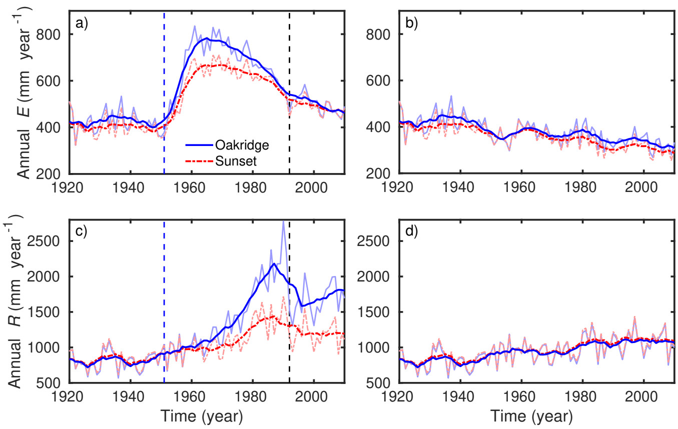

Figure 11: Annual (lighter curves) and 10-year running mean (bold curves). (a, b) Evaporation (E) and (c, d) runoff (R) for the (a, c) base run and (b, d) no irrigation run over the study period. Start of the irrigation period (1951, blue vertical-dashed line) and start of irrigation restrictions (1992, black vertical-dashed line). Adapted from **Paper III**.

found and used to determine the reasonable amount of irrigation using EC observations over irrigated urban lawns (e.g. Danielson et al., 1980). The residents in Vancouver do not pay based on consumption of water but a fixed amount and therefore the irrigation restrictions are important control mechanism. Using different combinations of irrigation restrictions in model runs, a stricter restriction (irrigation allowed once per week) can be recommended, which would allow sufficient amount of water for the gardens, but it would prevent the excess irrigation occurring especially in the more prosperous Oakridge (up to 956 mm year^{-1} with current restrictions).

Without irrigation, evaporation and runoff would have had rather similar linear trends due to urbanization and densification at both study sites: decreasing trend in evaporation of 1.3 and 1.4 mm year^{-1} increasing trend in runoff of 3.9 and 4.0 mm year^{-1} in Oakridge and Sunset, respectively (Figure 11). The effects of urbanization and densification on runoff are further analysed by the dependence of annual runoff coefficients (runoff normalised with precipitation) on the annual precipitation in three decade long development periods to understand how the coefficients have changed: early stage of urbanization (1921–1930), middle (1961–1971), and mature (2001–2010). There is a

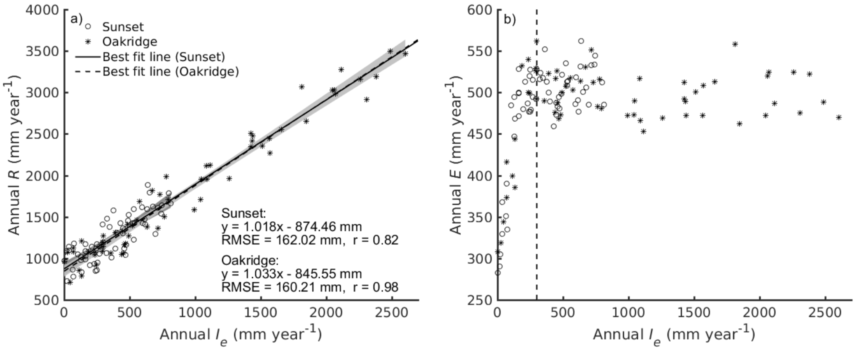

Figure 12: Annual (a) runoff (R) and (b) evaporation (E) as a function of irrigation (I_e). The grey areas are nonsimultaneous functional bounds with 95% cinfidence level. The vertical dashed line is the 300-mm threshold after which the excess water will go to R and not to E. Adapted from **Paper III**.

clear increase in the runoff coefficients over each decade (i.e. more runoff produced from precipitation) (Figure 13). The differences between the fit lines for early and middle phase of urbanisation are due to the initial urbanisation, but the differences between the fit lines for middle and mature phase of urbanisation are due to the densification especially in Oakridge since all the current built lots were developed by the mid-1950s and the densification is due to the building of larger garages, terraces and driveways and expanded houses (Figure 6). The impact of densification increases the runoff coefficient approximately as much as the initial urbanisation even though the increase of impervious fraction is much smaller: change in impervious cover fraction up to 0.4 and up to 0.48 due to urbanisation in Oakridge and Sunset, respectively; and up to 0.13 and up to 0.20 due to densification. The increase of annual runoff coefficients are 0.057 and 0.060 due to urbanisation in Oakridge and Sunset, respectively; and 0.060 and 0.067 due to densification, calculated from the differences of the medians of these decade long urbanisation phases. This is because the infiltration capacity is filled more rapidly when the fraction of pervious surfaces is decreasing. The initial urbanisation already induced large amount of impervious surfaces and therefore the small increase of impervious surfaces induced by densification fills the infiltration capacity of the remaining pervious surfaces more rapidly and more of the incoming water will go to runoff. This indicates that the densification has a substantial effect on the urban hydrological cycle even though its effect is often neglected when estimating the effect

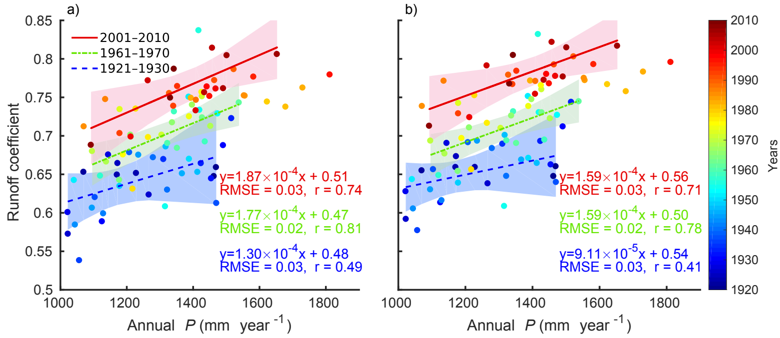

Figure 13: Annual runoff coefficients (colored dots) as a function of precipitation (P) for the no irrigation run in (a) Oakridge and (b) Sunset neighbourhoods in three development periods: 1921–1930 (early), 1961–1970 (middle), and 2001–2010 (mature). The shaded areas are nonsimultaneous functional bounds with 95% confidence level. See section 3.6 for statistics explanation. Adapted from **Paper III**.

of urban development on the local hydrological conditions.

The severe air pollution in Beijing affects the local scale urban hydrological cycle especially during small daily precipitation totals (**Paper IV**). The air pollution attenuates the incoming solar radiation by 167 W m^{-2} when comparing with cleaner conditions (comparison of medians of midday $K{\downarrow}$ of fairly clean conditions and extremely polluted conditions, see **Paper IV** for explanation of air quality levels). This reduces surface energy availability and evaporation by 0.42 mm day^{-1} (comparison of daily median of fairly clean conditions and extremely polluted conditions; t-test *p-value* $\ll 0.01$; Figure 14f). However, the effect of for example vapour pressure deficit and changes in soil water storage (i.e. availability of water) are not taken into account here and the changes in the water balance are assumed to be caused solely by the reduced incoming solar radiation.

Due to the decreased evaporation that modifies the water balance, the runoff coefficient increases. During the most polluted days with lowest precipitation (0–25 percentiles of daily precipitation totals) the runoff coefficient is largest on the daily median (0.097) whereas significantly lower (0.039–0.049; t-test *p-value* from $\ll 0.01$ to <0.05) during the cleaner conditions when the air quality is stratified into four quantiles (**Paper IV**). The higher amount of P during the cleaner days starts to dominate as the higher daily

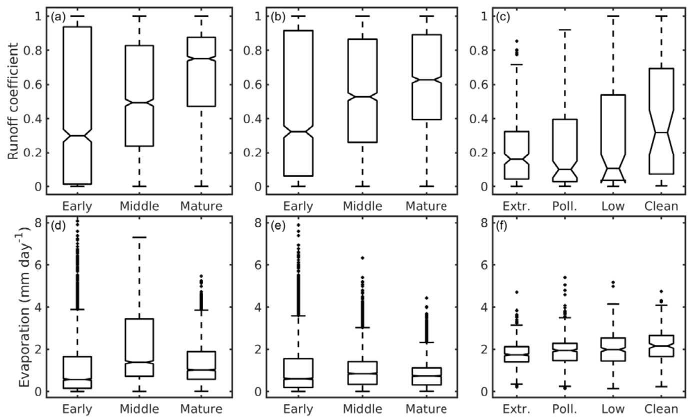

Figure 14: Box plot for (a–c) runoff coefficient from daily cumulative values and (d–f) daily cumulative evaporation stratified by level of urbanization for (a,d) Oakridge and (b,e) Sunset and by level of pollution for (c,f) Beijing. The early stage of urbanization is period 1921–1930, middle 1961–1970 and mature 2001–2010. The pollution levels are extremely polluted (AOD>1), polluted (0.438–1), low pollution (0.203–0.438) and fairly clean air (<0.203). The notches indicate the 95% confidence levels.

precipitation totals are included in the analysis. When all the precipitation events are included, the runoff coefficient during the cleaner conditions is significantly highest (0.30, t-test *p-value* <0.05) and stays rather similar with other air quality levels (0.16, 0.10, 0.10 for extremely polluted air, polluted air and low pollution conditions; Figure 14c). The small increase in runoff coefficient during small daily precipitation totals may not affect flooding substantially, but as the top urban soil layers are heavily polluted in gardens, roadsides and residential areas in Beijing (e.g. Chen et al., 2005; Xia et al., 2011), the surface runoff water has been shown to include significantly more pollutants than rain water (Yufen et al., 2008). Therefore the hypothesis is that even the small increase in runoff could presumably flush more of these pollutants from the surfaces to urban water bodies. Decreased evaporation with poorer air quality is also assumed to increase drainage (0.50–0.70 mm day^{-1} from fairly clean conditions to extremely polluted conditions, t-test *p-value* for increase: $\ll 0.01$) potentially causing more infiltration to groundwater from surfaces on occasions where higher atmospheric deposition had occurred. Thus, potentially increasing the pollutant loads.

Direct comparison of the results from Vancouver and Beijing is challenging due to different climate conditions and different types of urban areas (LCZ 6 and LCZ 1, respectively). However, based on the results (Figure 14), in general the effect of haze on local scale urban hydrological cycle is presumably much smaller than the effects of urbanisation, densification and increased irrigation and therefore its effect is less substantial for urban hydrology.

The increase of daily runoff coefficient due to urban development over the study period is 0.45 in Oakridge and 0.30 in Sunset (comparison of the medians of early and mature phase; Figure 14). The dominant effect of irrigation is evident in the daily cumulative evaporation especially in Oakridge (Figure 14). The median evaporation during the early phase, before irrigation has started, is at its lowest (0.56 mm day^{-1}) and at its highest during the middle phase (1.38 mm day^{-1}) when the irrigation has met the threshold, which after the effect of urbanisation, densification and irrigation restrictions start to decrease it leading to evaporation of 1.02 mm day^{-1} during the mature phase. The total change in evaporation due to urban development is 0.45 and 0.14 mm day^{-1} in Oakridge and Sunset, respectively (comparison of the medians of early and mature phase).

The changes in daily cumulative evaporation due to urban development and air quality are 30%, 14% and 21% in Oakridge, Sunset and Beijing, respectively, from the mean daily evaporation (t-test *p-values* $\ll 0.01$). The systematic error in EC observations of latent heat flux is 8% and random error 18% (**Paper I**), and the changes induced are close to the error limits of observations. This also emphasises the importance of the numerical modelling in studying the subtle effects of the factors affecting the hydrological cycle in urban environments, as it is possible to isolate certain effects and study in detail the individual phenomena.

5 Broader impacts and applications

The improved understanding in factors affecting urban hydrological cycle obtained in this thesis can aid urban developers to estimate the changes induced by the urban development on local scale urban hydrological cycle. Especially the subsequent densification, which often occurs without further planning after the initial urbanisation, is often neglected by the urban developers. However, the results show that the effect of densification on increased runoff is as substantial as the initial urbanisation. Therefore it should be considered when designing sewer network for residential areas as otherwise the pipe capacity might not be sufficient in the future after the densification of the area.

In addition, an irrigation threshold which after garden irrigation does not benefit garden areas in Vancouver was identified. A stricter irrigation regulation, which still would allow enough water for the gardens to stay healthy, can be designed based on the result. Similar method can be used also in other cities to determine the reasonable amount of irrigation needed for the garden areas.

The improved understanding of the effects of haze on local scale urban hydrological cycle provides important information for urban planners in highly polluted cities, since changes due to haze could potentially have substantial impacts on the local water cycle. Furthermore, the knowledge of the potential deterioration of urban water bodies is important to practitioners who are trying to solve the problems related to increasing pollutant loads in urban waters.

The used SUEWS model is part of the Urban Multi-scale Environmental Predictor (UMEP; Lindberg et al., 2018), which is an easy to use GIS-software based climate service tool designed for researchers and service providers. UMEP has also a built-in possibility to download and use WFDEI data as meteorological forcing. Therefore increased knowledge of the uncertainties in WFDEI data and the tested correction methods as well as evaluation of SUEWS made in this thesis, benefits also the UMEP developer and user communities.

The methods presented in this thesis can be applied globally and most of the data used are open access data with a good global coverage. However, a proper evaluation of the reanalysis data and SUEWS model parametrisation has to be performed when applied to climate conditions different of the study sites used in this thesis. Thus, further research is needed in different climate conditions in order to determine SUEWS model parametrisation suitable for various climates globally and to evaluate the quality of reanalysis data in different urban environments. However, the evaluation of the WFDEI data and SUEWS in varying conditions is hard due to the lack of comprehensive observations in urban areas. Therefore also more urban observations are needed globally to increase the understanding and usability of the methods used in this thesis in varying conditions.

6 Review of papers and the author's contribution

This thesis consists of four research papers (Figure 15). The uncertainties in EC observations that are commonly used in evaluation of land surface models are examined in **Paper I**. The downscaling and correction of reanalysis data and evaluation of SUEWS using eddy covariance observations are examined in **Papers II and IV**. The factors affecting the local scale urban hydrological cycles are examined in **Papers III and IV** using SUEWS with corrected reanalysis forcing data. The author was taking part in planning of the research entity and individual papers. The author is solely responsible for the summary part of this thesis.

Paper I is the first study to characterise the representativeness of single-point eddy covariance flux observations in a densely built urban area in central Helsinki using a combination of two identical EC systems close to each other. Using this method the uncertainties in urban EC observations are examined and the obtained results can be used as a rule of thumb when evaluating in general the representativeness of urban EC measurements. The author was responsible for the measurements and contributed in writing the manuscript.

Paper II evaluates SUEWS performance using downscaled reanalysis data against eddy covariance observations in two cities (Vancouver and London) with different urban structures and climate conditions. Sensitivity tests of each meteorological variable of reanalysis data are assessed. Special attention is given to the downscaling of precipitation, since the results show that it is one of the most crucial variables in hydrological modelling. The author contributed to the development of the downscaling code and made most of the analyses and was also the main responsible for model runs and writing the paper.

Paper III investigates for the first time in detail the most important factors affecting local scale suburban water balance in Vancouver over a long period (1920-2010) via determining the relative contributions of the impacts of land cover changes and irrigation. This study is also the first to examine the effects of densification on urban hydrological cycle at the scale of individual lots and buildings. The author was the main responsible for determining the surface characteristics of the study areas, model runs, analysing the results and writing the paper.

Paper IV evaluates WATCH reanalysis data variables most crucial for hydrological modelling in highly polluted urban environment in Beijing. Correction method for incoming solar radiation is developed and evaluated using observations from the study area. In addition SUEWS performance is evaluated using eddy covariance observations. The effect of haze on local scale urban hydrological cycle is analysed using SUEWS forced with corrected WATCH meteorological reanalysis data. The author was the main responsible in development of the correction for accounting for the effect of haze, model runs, the analyses of the results and writing the paper.

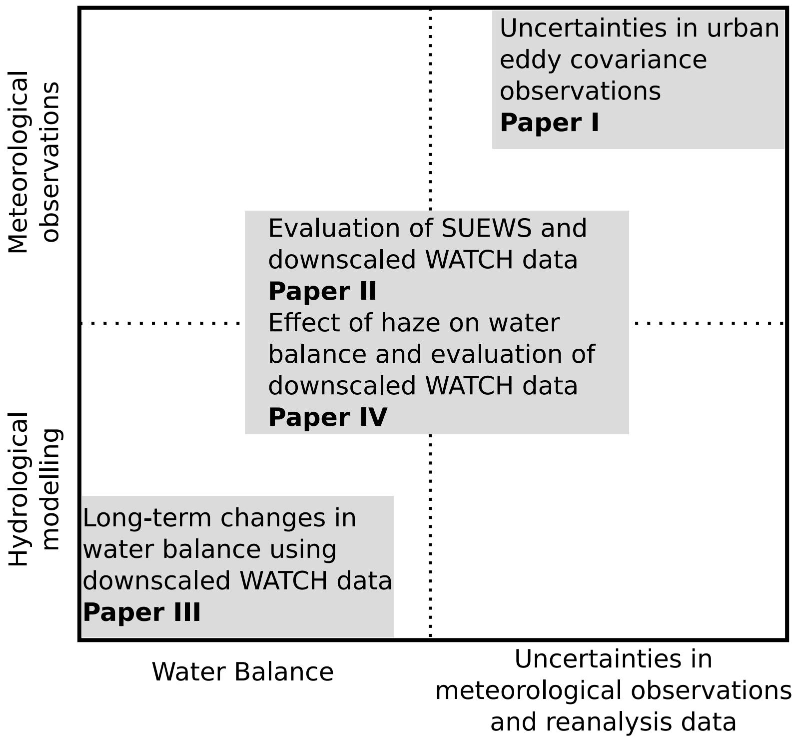

Figure 15: Relations of the papers to the studied aspects. The location of the gray boxes indicate how the paper contributes on the topics.

7 Conclusions

This thesis provides some of the first analyses of the dominant factors in the local scale urban hydrological cycle by isolating individual processes to examine their relative contribution to the urban water balance. The EC observations are commonly used to evaluate the land surface models which emphasises the importance of understanding the error sources in the observations. Thus, the uncertainties in urban EC measurements are analysed. Urban hydrological and land surface models require high resolution meteorological forcing data which are often lacking for the period of interest or at the required spatial and temporal resolution. Reanalysis products can help by providing the needed meteorological forcing, but proper evaluation and downscaling of the crucial variables have to be made prior to usage of the data.

In this thesis **Paper I** analyses the uncertainties in eddy covariance measurements in order to increase the understanding of its representativeness of the processes in the underlying source area. The results show that latent heat flux is one of the most uncertain variables to observe using this technique in urban environments. In addition, single observation system installed in a non-ideal location, often used in urban environments, leads to an underestimation of 8% in annual cumulative latent heat flux. This has to be taken into account when evaluating the urban models using the EC observations or analysing the subtle changes in urban hydrological cycle due to urban development processes using EC technique. However, these errors are slightly larger, but in the same magnitude as above vegetated environments. Thus the urban single-point observations can provide useful and representative measurements even when the location of the EC system is non-ideal.

The WFDEI reanalysis data are assessed as an input data to an urban energy and water balance model SUEWS in **Papers II and IV**, and the most crucial variables for correction are identified. From the sensitivity tests performed in **Paper II**, it is clear that the precipitation has the largest impact on the modelled evaporation and runoff in rather clear environments of Vancouver and London, while the incoming solar radiation has largest biases in the polluted environment of Beijing (**Paper IV**). The bias correction using quantile mapping (BCQM) applied for the WFDEI precipitation decreases the overestimation of the modelled evaporation and runoff in Vancouver and London. Since the effect of air pollution is not properly accounted for in WFDEI data, a correction method is applied and evaluated. The corrected WFDEI data represent meteorological conditions well also in highly polluted Beijing.

In **Paper III** the SUEWS model forced with corrected WATCH reanalysis data, which are evaluated in **Paper II**, are used in long-term analysis of urban hydrological cycle in two suburban areas, Oakridge and Sunset, in Vancouver. The whole lifespan of the two areas is examined from prior to urban development (1920) to when the areas are fully developed modern day inner city suburban areas (2010). Garden irrigation has the dominant impact on the suburban hydrological cycle over urbanisation and densification. Annually surface runoff is linearly dependent on the amount of irrigation, whereas evaporation increases linearly to a threshold value of approximately 300 mm year^{-1} of irrigation, which after the excess water is going to runoff and does not benefit the garden areas. Based on the results in **Paper III**, stricter irrigation restrictions could be recommended, which would provide enough water for the garden areas, but would prevent the excessive water use.

Furthermore, urbanisation and densification have substantially increased the runoff coefficients. The impact of densification increases the runoff coefficient as much as the initial urbanisation even though the increase of impervious surfaces is substantially smaller due to densification. However, the effect of densification on hydrological cycle is often neglected by the urban planners.

The detailed analysis of water balance terms finds that atmospheric pollution attenuates $K\downarrow$, which is expected to modify the water balance. The evaporation is decreasing with the increasing air pollution, which increases runoff and soil infiltration especially during smaller precipitation totals. The hypothesis is that this is expected to flush pollutants from polluted surfaces and top layers of soil which leads to increased pollutant loads in urban water bodies which are already poor in Beijing.

This thesis is the first study to examine the quality of WATCH reanalysis data in local scale urban environment and to apply the needed corrections. This is also the first to examine in detail the effects of different urban development processes on the local scale urban hydrological cycle enabled by the hydrological simulations over the whole life-span of residential areas in Vancouver and over a decade in a dense city centre in polluted Beijing.

The improved understanding brings valuable information for urban planning allowing the design of sustainable cities that can adapt and mitigate to the challenges induced by urban development. In addition, the uncertainties of urban EC observations are analysed for the first time and the results can be used as a rule of thumb when evaluating the representativeness of urban EC observations. The land surface, ecosystem and adaptation modelling communities as a whole benefit of the improved understanding of the uncertainties of reanalysis data and the downscaling methods used. In addition, the most direct benefit of the results and methods of this thesis is for the SUEWS modelling, other land surface modelling and micrometeorological research communities, due to the improved understanding of the evaluation of the models, the factors affecting the urban hydrological cycle and the uncertainties and representativeness of the urban EC observations. The methods presented in this thesis can be applied globally and most of the data used are open access data with a good global coverage.

References

Alexander, P. J., Mills, G., and Fealy, R. (2015). Using LCZ data to run an urban energy balance model. *Urban Climate*, 13.

Anandakumar, K. (1999). A study on the partition of net radiation into heat fluxes on a dry asphalt surface. *Atmos. Environ.*, 33(24):3911–3918.

Ao, X., Grimmond, C. S. B., Chang, Y., Liu, D., Tang, Y., Hu, P., Wang, Y., Zou, J., and Tan, J. (2016). Heat, water and carbon exchanges in the tall megacity of Shanghai: challenges and results. *Int. J. Climatol.*, 36(14):4608–4624.

Arnfield, A. J. (2003). Two decades of urban climate research: a review of turbulence, exchanges of energy and water, and the urban heat island. *Int. J. Climatol.*, 23(1):1–26.

Asaeda, T. and Ca, V. T. (1993). The subsurface transport of heat and moisture and its effect on the environment: A numerical model. *Bound.-Layer Meteor.*, 65(1):159–179.

Aubinet, M., Vesala, T., and Papale, D., editors (2012). *Eddy Covariance - A Practical Guide to Measurement and Data Analysis.* Springer Atmospheric Sciences, the Netherlands.

Auvinen, M., Järvi, L., Hellsten, A., Rannik, U., and Vesala, T. (2017). Numerical framework for the computation of urban flux footprints employing large-eddy simulation and lagrangian stochastic modeling. *Geosci. Model Dev.*, 10(11):4187–4205.

Baklanov, A., Grimmond, C., Carlson, D., Terblanche, D., Tang, X., Bouchet, V., Lee, B., Langendijk, G., Kolli, R., and Hovsepyan, A. (2018). From urban meteorology, climate and environment research to integrated city services. *Urban Climate*, 23:330–341. ICUC9: The 9th International Conference on Urban Climate.

Baldocchi, D. D., Hincks, B. B., and Meyers, T. P. (1988). Measuring biosphere-atmosphere exchanges of biologically related gases with micrometeorological methods. *Ecology*, 69(5):1331–1340.

Barlow, J. F. (2014). Progress in observing and modelling the urban boundary layer. *Urban Climate*, 10:216–240.

Barlow, J. F., Harrison, J., Robins, A. G., and Wood, C. R. (2011). A wind-tunnel study of flow distortion at a meteorological sensor on top of the BT Tower, London, UK. *J. Wind Eng. Ind. Aerod.*, 99(9):899–907. 9th UK Conference on Wind Engineering (September, 2010).

Bastola, S. and Misra, V. (2014). Evaluation of dynamically downscaled reanalysis precipitation data for hydrological application. *Hydrol. Process.*, 28(4):1989–2002.

Beijing Municipal Bureau of Statistics (2016). Beijing statistical yearbook. Accessed 3 Oct 2018.

Best, M. J. and Grimmond, C. S. B. (2015). Key conclusions of the first international urban land surface model comparison project. *Bull. Amer. Meteor. Soc.*, 96(5):805–819.

Best, M. J. and Grimmond, C. S. B. (2016). Modelling the partitioning of turbulent fluxes at urban sites with varying vegetation cover. *J. Hydrometeorol.*, 17:2537–2553.

Brümmer, B., Lange, I., and Konow, H. (2012). Atmospheric boundary layer measurements at the 280 m high Hamburg weather mast 1995-2011: mean annual and diurnal cycles. *Meteor. Z.*, 21(4):319–335.

Cai, W., Li, K., Liao, H., Wang, H., and Wu, L. (2017). Weather conditions conducive to Beijing severe haze more frequent under climate change. *Nature Climate Change*, 7:257–263.

Cao, C., Lee, X., Liu, S., Schultz, N., Xiao, W., Zhang, M., and Zhao, L. (2016). Urban heat islands in China enhanced by haze pollution. *Nature communications*, 7:12509.

Che, H., Zhang, X., Chen, H., Damiri, B., Goloub, P., Li, Z., Zhang, X., Wei, Y., Zhou, H., Dong, F., Li, D., and Zhou, T. (2009). Instrument calibration and aerosol optical depth validation of the China Aerosol Remote Sensing Network. *J. Geophys. Res. Atmos.*, 114.

Chen, H. and Wang, H. (2015). Haze days in north China and the associated atmospheric circulations based on daily visibility data from 1960 to 2012. *J. Geophys. Res. Atmos.*, 120(12):5895–5909.

Chen, T.-B., Zheng, Y.-M., Lei, M., Huang, Z.-C., Wu, H.-T., Chen, H., Fan, K.-K., Yu, K., Wu, X., and Tian, Q.-Z. (2005). Assessment of heavy metal pollution in surface soils of urban parks in Beijing, China. *Chemosphere*, 60(4):542–551.

Christen, A., Coops, N., Crawford, B., Kellett, R., Liss, K., Olchovski, I., Tooke, T., van der Laan, M., and Voogt, J. (2011). Validation of modeled carbon-dioxide emissions from an urban neighborhood with direct eddy-covariance measurements. *Atmos. Environ.*, 45(33):6057–6069.

Cleveland, W. S. (1979). Robust locally weighted regression and smoothing scatterplots. *J. Am. Stat. Assoc.*, 74(368):829–836.

Cleveland, W. S. (1981). LOWESS: A program for smoothing scatterplots by robust locally weighted regression. *The American Statistician*, 35(1):54.

Cohen, A. J., Brauer, M., Burnett, R., Anderson, H. R., Frostad, J., Estep, K., Balakrishnan, K., Brunekreef, B., Dandona, L., Dandona, R., Feigin, V., Freedman, G., Hubbell, B., Jobling, A., Kan, H., Knibbs, L., Liu, Y., Martin, R., Morawska, L., Pope, C. A., Shin, H., Straif, K., Shaddick, G., Thomas, M., van Dingenen, R., van Donkelaar, A., Vos, T., Murray, C. J. L., and Forouzanfar, M. H. (2017). Estimates and 25-year trends of the global burden of disease attributable to ambient air pollution: an analysis of data from the global burden of diseases study 2015. *The Lancet*, 389(10082):1907–1918.

Coppin, P. A. and Taylor, K. J. (1983). A three-component sonic anemometer/thermometer system for general micrometeorological research. *Bound.-Layer Meteor.*, 27(1):27–42.

Danielson, R. E., Hart, W. E., Feldhake, C. M., and Haw, P. M. (1980). Water requirements for urban lawns in Colorado. Completion report No. 97, Colorado State University.

Dee, D. P., Uppala, S. M., Simmons, A. J., Berrisford, P., Poli, P., Kobayashi, S., Andrae, U., Balmaseda, M. A., Balsamo, G., Bauer, P., Bechtold, P., Beljarrs, A. C. M., van de Berg, L., Bidlot, J., Bormann, N., Delsol, C., Dragani, R., Fuentes, M., Geer, A. J., Haimberger, L., Healy, S. B., Hersbach, H., Hólm, E. V., Isaksen, L., Kållberg, P., Köhler, M., Matricardi, M., McNally, A. P., Monge-Sanz, B. M., Morcrette, J.-J., Park, B.-K., Peubey, C., de Rosnay, P., Tavolato, C., Thépaut, J.-N., and Vitart, F. (2011). The ERA-Interim reanalysis: Configuration and performance of the data assimilation system. *Quart. J. Roy. Meteor. Soc.*, 137:553–597.

Demuzere, M., Coutts, A. M., Göhler, M., Broadbent, A. M., Wouters, H., van Lipzig, N. P. M., and Gebert, L. (2014). The implementation of biofiltration systems, rainwater tanks and urban irrigation in a single-layer urban canopy model. *Urban Climate*, 10(Part 1):148–170.

Demuzere, M., Harshan, S., Järvi, L., Roth, M., Grimmond, C. S. B., Masson, V., Oleson, K. W., Velasco, E., and Wouters, H. (2017). Impact of urban canopy models and external parameters on the modelled urban energy balance in a tropical city. *Quart. J. Roy. Meteor. Soc.*, 143(704):1581–1596.

Domrös, M. and Peng, G. (1988). *The climate of China*. Springer-Verlag Berlin Heidelberg.

Dosio, A. and Paruolo, P. (2011). Bias correction of the ENSEMBLES high-resolution climate change projections for use by impact models: Evaluation on the present climate. *J. Geophys. Res. Atmos.*, 116(D16):D16106.

Essou, G. R. C., Sabarly, F., Lucas-Picher, P., Brissette, F., and Poulin, A. (2016). Can precipitation and temperature from meteorological reanalyses be used for hydrological modeling? *J. Hydrometeorol.*, 17(7):1929–1950.

Fan, J., Rosenfeld, D., Yang, Y., Zhao, C., Leung, L. R., and Li, Z. (2015). Substantial contribution of anthropogenic air pollution to catastrophic floods in Southwest China. *Geophys. Res. Lett.*, 42(14):6066–6075.

Fowler, H. J., Blenkinsop, S., and Tebaldi, C. (2007). Linking climate change modelling to impacts studies: recent advances in downscaling techniques for hydrological modelling. *Int. J. Climatol.*, 27(12):1547–1578.

Früh, B., Becker, P., Deutschländer, T., Hessel, J.-D., Kossmann, M., Mieskes, I., Namyslo, J., Roos, M., Sievers, U., Steigerwald, T., Turau, H., and Wienert, U. (2011). Estimation of climate-change impacts on the urban heat load using an urban climate model and regional climate projections. *J. Appl. Meteorol. Clim.*, 50(1):167–184.

Gober, P., Brazel, A., Quay, R., Myint, S., Grossman-Clarke, S., Miller, A., and Rossi, S. (2009). Using watered landscapes to manipulate urban heat island effects: How much water will it take to cool Phoenix? *Journal of the American Planning Association*, 76(1):109–121.

Gooré Bi, E., Gachon, P., Vrac, M., and Monette, F. (2017). Which downscaled rainfall data for climate change impact studies in urban areas? Review of current approaches and trends. *Theor. Appl. Climatol.*, 127(3):685–699.

Greater London Authority (2015). Daytime population, borough. Created 25 Nov 2013, (modified 7 Oct 2015), accessed 1 Mar 2016.

Grimmond, C., Cleugh, H., and Oke, T. (1991). An objective urban heat storage model and its comparison with other schemes. *Atmos. Environ. B.-Urb.*, 25(3):311–326.

Grimmond, C., King, T., Cropley, F., Nowak, D., and Souch, C. (2002). Local-scale fluxes of carbon dioxide in urban environments: methodological challenges and results from Chicago. *Environ. Pollut.*, 116:S243–S254.

Grimmond, C., Roth, M., Oke, T., Au, Y., Best, M., Betts, R., Carmichael, G., Cleugh, H., Dabberdt, W., Emmanuel, R., Freitas, E., Fortuniak, K., Hanna, S., Klein, P., Kalkstein, L., Liu, C., Nickson, A., Pearlmutter, D., Sailor, D., and Voogt, J. (2010a). Climate and more sustainable cities: Climate information for improved planning and management of cities (producers/capabilities perspective). *Procedia Environ. Sci.*, 1:247–274. World Climate Conference - 3.

Grimmond, C. S. B. (2006). Progress in measuring and observing the urban atmosphere. *Theor. Appl. Climatol.*, 84(1):3–22.

Grimmond, C. S. B., Blackett, M., Best, M. J., Baik, J.-J., Belcher, S. E., Beringer, J., Bohnenstengel, S. I., Calmet, I., Chen, F., Coutts, A., Dandou, A., Fortuniak, K., Gouvea, M. L., Hamdi, R., Hendry, M., Kanda, M., Kawai, T., Kawamoto, Y., Kondo, H., Krayenhoff, E. S., Lee, S.-H., Loridan, T., Martilli, A., Masson, V., Miao, S., Oleson, K., Ooka, R., Pigeon, G., Porson, A., Ryu, Y.-H., Salamanca, F., Steeneveld, G. J., Tombrou, M., Voogt, J. A., Young, D. T., and Zhang, N. (2011). Initial results from phase 2 of the international urban energy balance model comparison. *International Journal of Climatology*, 31(2):244–272.

Grimmond, C. S. B., Blackett, M., Best, M. J., Barlow, J., Baik, J.-J., Belcher, S. E., Bohnenstengel, S. I., Calmet, I., Chen, F., Dandou, A., Fortuniak, K., Gouvea, M. L., Hamdi, R., Hendry, M., Kawai, T., Kawamoto, Y., Kondo, H., Krayenhoff, E. S., Lee, S.-H., Loridan, T., Martilli, A., Masson, V., Miao, S., Oleson, K., Pigeon, G., Porson, A., Ryu, Y.-H., Salamanca, F., Shashua-Bar, L., Steeneveld, G.-J., Tombrou, M., Voogt, J., Young, D., and Zhang, N. (2010b). The international urban energy balance models comparison project: First results from phase 1. *J. Appl. Meteorol. Clim.*, 49(6):1268–1292.

Grimmond, C. S. B. and Oke, T. R. (1986). Urban water balance: 2. results from a suburb of Vancouver, British Columbia. *Water Resour. Res.*, 22(10):1404–1412.

Grimmond, C. S. B. and Oke, T. R. (1991). An evapotranspiration-interception model for urban areas. *Water Resour. Res.*, 27(7):1739–1755.

Grimmond, C. S. B. and Oke, T. R. (1999). Aerodynamic properties of urban areas derived from analysis of surface form. *J. Appl. Meteor.*, 38(9):1262–1292.

Grimmond, C. S. B., Oke, T. R., and Steyn, D. G. (1986). Urban water balance: 1. a model for daily totals. *Water Resour. Res.*, 22(10):1397–1403.

Hanafusa, T., Fujitani, T., Kobori, Y., and Mitsuta, Y. (1982). A new type sonic anemometer-thermometer for field operation. *Pap. Meteor. Geophys.*, 33(1):1–19.

Harris, I., Jones, P., Osborn, T., and Lister, D. (2014). Updated high-resolution grids of monthly climatic observations – the CRU TS3.10 dataset. *Int. J. Climatol.*, 34(3):623–642.

Hirsch, R. M., Slack, J. R., and Smith, R. A. (1982). Tecniques of trend analysis for monthly water quality data. *Water Resour. Res.*, 18(1).

Hollinger, D. Y. and Richardson, A. D. (2005). Uncertainty in eddy covariance measurements and its application to physiological models. *Tree Physiol.*, 25(7):873–885.

IPCC (2014). Climate change 2014: impacts, adaptation, and vulnerability. Part A: global and sectoral aspects. In Field, C., Barros, V., Dokken, D., Mach, K., Mastrandrea, P., and White, L., editors, *Contribution of Working Group II to the Fifth Assessment Report of the Intergovernmental Panel on Climate Change*. Cambridge University Press, Cambridge, United Kindom and New York, NY, USA.

Jacobson, M. Z. (1998). Studying the effects of aerosols on vertical photolysis rate coefficient and temperature profiles over an urban airshed. *J. Geophys. Res. Atmos.*, 103(D9):10593–10604.

Järvi, L., Grimmond, C. S. B., McFadden, J. P., Christen, A., Strachan, I. B., Taka, M., Warsta, L., and Heimann, M. (2017). Warming effects on the urban hydrology in cold climate regions. *Scientific Reports*, 7:5833.

Järvi, L., Grimmond, C. S. B., Taka, M., Nordbo, A., Setälä, H., and Strachan, I. B. (2014). Development of the Surface Urban Energy and Water Balance Scheme (SUEWS) for cold climate cities. *Geosci. Model Dev.*, 7:1691–1711.

Järvi, L., Grimmond, S., and Christen, A. (2011). The Surface Urban Energy and Water Balance Scheme (SUEWS): Evaluation in Los Angeles and Vancouver. *J. Hydrol.*, 411:219–237.

Jia, H., Lu, Y., Yu, S. L., and Chen, Y. (2012). Planning of LID-BMPs for urban runoff control: The case of Beijing Olympic Village. *Sep. Purif. Technol.*, 84:112–119.

Jongman, B., Hochrainer-Stigler, S., Feyen, L., Aerts, J. C. J. H., Mechler, R., Botzen, W. J. W., Bouwer, L. M., Pflug, G., Rojas, R., and Ward, P. J. (2014). Increasing stress on disaster-risk finance due to large floods. *Nat. Clim. Change*, 4:264–268.

Kajino, M., Ueda, H., Han, Z., Kudo, R., Inomata, Y., and Kaku, H. (2017). Synergy between air pollution and urban meteorological changes through aerosol-radiation-diffusion feedback–a case study of Beijing in January 2013. *Atmos. Environ.*, 171:98–110.

Kalanda, B. D., Oke, T. R., and Spittlehouse, D. L. (1980). Suburban energy balance estimates for Vancouver, B.C., using the Bowen ratio-energy balance approach. *J. Appl. Meteor.*, 19(7):791–802.

Kalnay, E., Kanamitsu, M., Kistler, R., Collins, W., Deaven, D., Gandin, L., Iredell, M., Saha, S., White, G., Woollen, J., Zhu, Y., Chelliah, M., Ebisuzaki, W., Higgins, W., Janowiak, J., Mo, K. C., Ropelewski, C., Wang, J., Leetmaa, A., Reynolds, R., Jenne, R., and Joseph, D. (1996). The NCEP/NCAR 40-year reanalysis project. *Bull. Amer. Meteor. Soc.*, 77(3):437–472.

Kan, H., Chen, R., and Tong, S. (2012). Ambient air pollution, climate change, and population health in China. *Environ. Int.*, 42:10–19.

Kanamitsu, M. and Kanamaru, H. (2007). Fifty-seven-year California reanalysis downscaling at 10 km (CaRD10). Part I: System detail and validation with observations. *J. Climate*, 20(22):5553–5571.

Karsisto, P., Fortelius, C., Demuzere, M., Grimmond, C. S. B., Oleson, K. W., Kouznetsov, R., Masson, V., and Järvi, L. (2016). Seasonal surface urban energy balance and wintertime stability simulated using three land-surface models in the high-latitude city Helsinki. *Quart. J. Roy. Meteor. Soc.*, 142(694):401–417.

Kellett, R., Christen, A., Coops, N. C., van der Laan, M., Crawford, B., Tooke, T. R., and Olchovski, I. (2013). A systems approach to carbon cycling and emissions modeling at an urban neighborhood scale. *Landscape Urban Plan.*, 110:48–58.

Kendall, M. G. (1975). *Rank Correlation Methods.* Charles Griffin, London.

Keogh, S., Mills, G., and Fealy, R. (2012). The energy budget of the urban surface: two locations in Dublin. *Irish Geography*, 45(1):1–23.

Kersalo, J. and Pirinen, P. (2009). Suomen maakuntien ilmasto (in finnish). Reports 2009:8, Finnish Meteorological Institute. 185 pages.

Kessomkiat, W., Franssen, H.-J. H., Graf, A., and Vereecken, H. (2013). Estimating random errors of eddy covariance data: An extended two-tower approach. *Agr. Forest Meteorol.*, 171–172:203–219.

Kobayashi, S., Ota, Y., Harada, Y., Ebita, A., Moriya, M., Onoda, H., Onogi, K., Kamahori, H., Kobayashi, C., Endo, H., Miyaoka, K., and Takahashi, K. (2015). The JRA-55 reanalysis: General specifications and basic characteristics. *J. Meteorol. Soc. Jpn. Ser. II*, 93(1):5–48.

Kondo, H., Genchi, Y., Kikegawa, Y., Ohashi, Y., Yoshikado, H., and Komiyama, H. (2005). Development of a multi-layer urban canopy model for the analysis of energy consumption in a big city: Structure of the urban canopy model and its basic performance. *Bound.-Layer Meteor.*, 116(3):395–421.

Kotthaus, S. and Grimmond, C. (2014a). Energy exchange in a dense urban environment – Part I: Temporal variability of long-term observations in central London. *Urban Climate*, 10:261–280. ICUC8: The 8th International Conference on Urban Climate and the 10th Symposium on the Urban Environment.

Kotthaus, S. and Grimmond, C. (2014b). Energy exchange in a dense urban environment – Part II: Impact of spatial heterogeneity of the surface. *Urban Climate*, 10:281–307. ICUC8: The 8th International Conference on Urban Climate and the 10th Symposium on the Urban Environment.

Kulmala, M. (2015). Atmospheric chemistry: China's choking cocktail. *Nature*, 526:497–499.

Kulmala, M. (2018). Build a global earth observatory. *Nature*, 553:21–23.

Kurek, W. and Ostfeld, A. (2013). Multi-objective optimization of water quality, pumps operation, and storage sizing of water distribution systems. *J. Environ. Manage.*, 115:189–197.

Kurppa, M., Nordbo, A., Haapanala, S., and Järvi, L. (2015). Effect of seasonal variability and land use on particle number and CO_2 exchange in Helsinki, Finland. *Urban Climate*, 13:94–109.

Kusaka, H., Kondo, H., Kikegawa, Y., and Kimura, F. (2001). A simple single-layer urban canopy model for atmospheric models: Comparison with multi-layer and slab models. *Bound.-Layer Meteor.*, 101(3):329–358.

Lee, J., Pak, G., Yoo, C., Kim, S., and Yoon, J. (2010). Effects of land use change and water reuse options on urban water cycle. *J. Environ. Sci.*, 22(6):923–928.

Lee, X., Massman, W., and Law, B., editors (2004). *Handbook of micrometeorology - A guide for surface flux measurement and analysis - Introduction*, volume 29. Kluwer Academic Publisher, the Netherlands.

Lelieveld, J., Evans, J. S., Fnais, M., Giannadaki, D., and Pozzer, A. (2015). The contribution of outdoor air pollution sources to premature mortality on a global scale. *Nature*, 525:367–371.

Lemonsu, A., Kounkou-Arnaud, R., Desplat, J., Salagnac, J.-L., and Masson, V. (2013). Evolution of the Parisian urban climate under a global changing climate. *Climatic Change*, 116(3).

Lenderink, G. and van Meijgaard, E. (2008). Increase in hourly precipitation extremes beyond expectations from temperature changes. *Nat. Geosci.*, 1:511–514.

Lenschow, D. H., Mann, J., and Kristensen, L. (1994). How long is long enough when measuring fluxes and other turbulence statistics? *J. Atmos. Oceanic Technol.*, 11(3):661–673.

Liang, X., Miao, S., Li, J., Bornstein, R., Zhang, X., Gao, Y., Chen, F., Cao, X., Cheng, Z., Clements, C., Dabberdt, W., Ding, A., Ding, D., Dou, J. J., Dou, J. X., Dou, Y., Grimmond, C. S. B., González-Cruz, J. E., He, J., Huang, M., Huang, X., Ju, S., Li, Q., Niyogi, D., Quan, J., Sun, J., Sun, J. Z., Yu, M., Zhang, J., Zhang, Y., Zhao, X., Zheng, Z., and Zhou, M. (2018). SURF: Understanding and predicting urban convection and haze. *Bull. Amer. Meteor. Soc.*, 99(7):1391–1413.

Lindberg, F., Grimmond, C., Gabey, A., Huang, B., Kent, C. W., Sun, T., Theeuwes, N. E., Järvi, L., Ward, H. C., Capel-Timms, I., Chang, Y., Jonsson, P., Krave, N., Liu, D., Meyer, D., Olofson, K. F. G., Tan, J., Wästberg, D., Xue, L., and Zhang, Z. (2018). Urban Multi-scale Environmental Predictor (UMEP): An integrated tool for city-based climate services. *Environ. Modell. Softw.*, 99:70–87.

Lins, H. F. and Slack, J. R. (1999). Streamflow trends in the United States. *Geophys. Res. Lett.*, 26(2):227–230.

Liu, H. Z., Feng, J. W., Järvi, L., and Vesala, T. (2012). Four-year (2006–2009) eddy covariance measurements of CO_2 flux over an urban area in Beijing. *Atmos. Chem. Phys.*, 12:7881–7892.

Mann, H. B. (1945). Nonparametric tests against trend. *Econometrica*, 13(3):245–259.

Martilli, A., Clappier, A., and Rotach, M. W. (2002). An urban surface exchange parameterisation for mesoscale models. *Bound.-Layer Meteor.*, 104(2):261–304.

Masson, V., Le Moigne, P., Martin, E., Faroux, S., Alias, A., Alkama, R., Belamari, S., Barbu, A., Boone, A., Bouyssel, F., Brousseau, P., Brun, E., Calvet, J.-C., Carrer, D., Decharme, B., Delire, C., Donier, S., Essaouini, K., Gibelin, A.-L., Giordani, H., Habets, F., Jidane, M., Kerdraon, G., Kourzeneva, E., Lafaysse, M., Lafont, S., Lebeaupin Brossier, C., Lemonsu, A., Mahfouf, J.-F., Marguinaud, P., Mokhtari, M., Morin, S., Pigeon, G., Salgado, R., Seity, Y., Taillefer, F., Tanguy, G., Tulet, P., Vincendon, B., Vionnet, V., and Voldoire, A. (2013). The SURFEXv7.2 land and ocean surface platform for coupled or offline simulation of earth surface variables and fluxes. *Geosci. Model Dev.*, 6(4):929–960.

Mayer, H. (1999). Air pollution in cities. *Atmos. Environ.*, 33(24):4029–4037.

McPherson, E. G., van Doorn, N. S., and Peper, P. J. (2016a). Urban tree database.

McPherson, E. G., van Doorn, N. S., and Peper, P. J. (2016b). Urban tree database and allometric equations. General technical report PSW-GTR-253, U.S. Department of Agriculture, Forest Service, Albany, CA.

Meierdiercks, K. L., Smith, J. A., Baeck, M. L., and Miller, A. J. (2010). Analyses of urban drainage network structure and its impact on hydrologic response. *J. Am. Water Resour. As.*, 46(5):932–943.

Met Office (2015). Meteorological data from Met Office. Accessed 17 November 2015.

Met Office (2016). Southern England: climate. Updated 11 Oct 2016, accessed 2 Oct 2018.

Miao, S., Dou, J., Chen, F., Li, J., and Li, A. (2012). Analysis of observations on the urban surface energy balance in Beijing. *Sci. China Earth Sci.*, 55(11):1881–1890.

Min, S.-K., Zhang, X., Zwiers, F. W., and Hegerl, G. C. (2011). Human contribution to more-intense precipitation extremes. *Nature*, 470:378–381.

Mitchell, V., Mein, R., and McMahon, T. (2001a). Modelling the urban water cycle. *Environ. Modell. Softw.*, 16(7):615–629.

Mitchell, V. G., McMahon, T. A., and Mein, R. G. (2003). Components of the total water balance of an urban catchment. *Environ. Manage.*, 32(6):735–746.

Mitchell, V. G., Mein, R. G., and McMahon, T. A. (2001b). Modelling the urban water cycle. *Environ. Modell. Softw.*, 16:615–629.

Molina, M. J. and Molina, L. T. (2004). Megacities and atmospheric pollution. *Journal of the Air & Waste Management Association*, 54(6):644–680.

Monteith, J. L. (1965). Evaporation and the environment. *Symp. Soc. Exp. Biol.*, 19:205–234.

Montgomery, R. B. (1948). Vertical eddy flux of heat in the atmosphere. *J. Meteor.*, 5(6):265–274.

Moriwaki, R., Kanda, M., Senoo, H., Hagishima, A., and Kinouchi, T. (2008). Anthropogenic water vapor emissions in Tokyo. *Water Resour. Res.*, 44:W11424.

Murto, S. (2017). *The impact of aerosols on the sensible and latent heat fluxes in Beijing*. Master's thesis, University of Helsinki.

Myrup, L. O. (1969). A numerical model of the urban heat island. *J. Appl. Meteor.*, 8(6):908–918.

Nordbo, A., Järvi, L., Haapanala, S., Moilanen, J., and Vesala, T. (2013). Intra-city variation in urban morphology and turbulence structure in Helsinki, Finland. *Bound.-Layer Meteor.*, 146(3):469–496.

Nordbo, A., Järvi, L., and Vesala, T. (2012). Revised eddy covariance flux calculation methodologies – effect on urban energy balance. *Tellus B*, 64(1).

Nordbo, A., Karsisto, P., Matikainen, L., Wood, C. R., and Järvi, L. (2015). Urban surface cover determined with airborne lidar at 2m resolution – implications for surface energy balance modelling. *Urban Climate*, 13:52–72.

Obropta, C. C. and Kardos, J. S. (2007). Review of urban stormwater quality models: Deterministic, stochastic, and hybrid approaches. *J. Am. Water Resour. As.*, 43(6):1508–1523.

Obukhov, A. M. (1951). Charakteristiki mikrostruktury vetra v prizemnom sloje atmosfery (characteristics of the micro-structure of the wind in the surface layer of the atmosphere). *Izv AN SSSR ser Geofiz*, 3:49–68.

O'Gorman, P. A. and Schneider, T. (2009). The physical basis for increases in precipitation extremes in simulations of 21st-century climate change. *Proc. Natl. Acad. Sci. USA*, 106(35):14773–14777.

Oke, T. and Hay, J. (1994). *The Climate of Vancouver*. Number 50 in B.C. geographical series. Department of Geography, University of British Columbia, 2nd edition.

Oke, T. R. (1979). Advectively-assisted evapotranspiration from irrigated urban vegetation. *Bound.-Layer Meteor.*, 17(2):167–173.

Oke, T. R. (1987). *Boundary layer climates*. Routledge, London, UK.

Oke, T. R. (1988). The urban energy balance. *Prog. Phys. Geog.*, 12(4):471–508.

Oke, T. R. (2008). Urban observations. In *Guide to meteorological instruments and methods of observation*, number WMO-No.8, chapter Part II–Observing systems, pages 765–793. World Meteorological Organization, Geneva, 8th edition.

Oke, T. R., Mills, G., Christen., A., and Voogt, J. A. (2017). *Urban Climates*. Cambridge University Press, Cambridge, UK.

Oleson, K. W., Bonan, G. B., Feddema, J., Vertenstein, M., and Grimmond, C. S. B. (2008). An urban parameterization for a global climate model. Part I: Formulation and evaluation for two cities. *J. Appl. Meteorol. Clim.*, 47(4):1038–1060.

Peña-Guzmán, C. A., Melgarejo, J., Prats, D., Torres, A., and Martínez, S. (2017). Urban water cycle simulation/management models: A review. *Water*, 9(4):285.

Pechlivanidis, I. G., Arheimer, B., Donnelly, C., Hundecha, Y., Huang, S., Aich, V., Samaniego, L., Eisner, S., and Shi, P. (2017). Analysis of hydrological extremes at different hydro-climatic regimes under present and future condition. *Climatic Change*, 141(3):467–481.

Peltola, O., Hensen, A., Marchesini, L. B., Helfter, C., Bosveld, F., van den Bulk, W., Haapanala, S., van Huissteden, J., Laurila, T., Lindroth, A., Nemitz, E., Röckmann, T., Vermeulen, A., and Mammarella, I. (2015). Studying the spatial variability of methane flux with five eddy covariance towers of varying height. *Agr. Forest Meteorol.*, 214–215:456–472.

Penman, H. L. (1948). Natural evaporation from open water, bare soil and grass. *P. Roy. Soc. Lond. A Mat.*, 193(1032):120–145.

Petäjä, T., Järvi, L., Kerminen, V.-M., Ding, A., Sun, J., Nie, W., Kujansuu, J., Virkkula, A., Yang, X., Fu, C., Zilitinkevich, S., and Kulmala, M. (2016). Enhanced air pollution via aerosol-boundary layer feedback in China. *Scientific Reports*, 6:18998.

Piani, C., Weedon, G., Best, M., Gomes, S., Viterbo, P., Hagemann, S., and Haerter, J. (2010). Statistical bias correction of global simulated daily precipitation and temperature for the application of hydrological models. *J. Hydrol.*, 395(3):199–215.

Post, H., Hendricks Franssen, H. J., Graf, A., Schmidt, M., and Vereecken, H. (2015). Uncertainty analysis of eddy covariance CO_2 flux measurements for different EC tower distances using an extended two-tower approach. *Biogeosciences*, 12(4).

Qin, H.-P., Li, Z.-X., and Fu, G. (2013). The effects of low impact development on urban flooding under different rainfall characteristics. *J. Environ. Manage.*, 129:577–585.

Räisänen, J. and Räty, O. (2013). Projections of daily mean temperature variability in the future: cross-validation tests with ENSEMBLES regional climate simulations. *Climate Dyn.*, 41(5):1553–1568.

Ramamurthy, P. and Bou-Zeid, E. (2014). Contribution of impervious surface to urban evaporation. *Water Resour. Res.*, 50:2889–2902.

Räty, O., Räisänen, J., and Ylhäisi, J. S. (2014). Evaluation of delta change and bias correction methods for future daily precipitation: intermodel cross-validation using ENSEMBLES simulations. *Climate Dyn.*, 42(9):2287–2303.

Raupach, M. R., Antonia, R. A., and Rajagopalan, S. (1991). Rough-wall turbulent boundary layers. *Applied Mechanics Reviews*, 44(1):1–25.

Rienecker, M. M., Suarez, M. J., Gelaro, R., Todling, R., Bacmeister, J., Liu, E., Bosilovich, M. G., Schubert, S. D., Takacs, L., Kim, G.-K., Bloom, S., Chen, J., Collins, D., Conaty, A., da Silva, A., Gu, W., Joiner, J., Koster, R. D., Lucchesi, R., Molod, A., Owens, T., Pawson, S., Pegion, P., Redder, C. R., Reichle, R., Robertson, F. R., Ruddick, A. G., Sienkiewicz, M., and Woollen, J. (2011). MERRA: NASA's modern-era retrospective analysis for research and applications. *J. Climate*, 24(14):3624–3648.

Rodriguez, F., Andrieu, H., and Creutin, J.-D. (2003). Surface runoff in urban catchment: morphological identification of unit hydrographs from urban databanks. *J. Hydrol.*, 283:146–168.

Rossman, L. (1993). EPANET water quality model. EPA/600/A-93/226 (NTIS PB93236552), U.S. Environmental Protection Agency, Washington, D.C.

Rossman, L. A. (2015). Storm Water Management Model user's manual version 5.1. EPA/600/R-14/413b, U.S. Environmental Protection Agency, Cincinnati, OH.

Rotach, M. W. (1999). On the influence of the urban roughness sublayer on turbulence and dispersion. *Atmos. Environ.*, 33(24):4001–4008.

Roth, M. (2000). Review of atmospheric turbulence over cities. *Quart. J. Roy. Meteor. Soc.*, 126(564):941–990.

Schneider, U., Becker, A., Finger, P., Meyer-Christoffer, A., Ziese, M., and Rudolf, B. (2013). GPCC's new land surface precipitation climatology based on quality-controlled in situ data and its role in quantifying the global water cycle. *Theor. Appl. Climatol.*, 115:15–40.

Shang, F., Uber, J. G., and Rossman, L. A. (2008). Modeling reaction and transport of multiple species in water distribution systems. *Environ. Sci. Technol.*, 42(3):808–814.

Sharma, A. K., Gray, S., Diaper, C., Liston, P., and Howe, C. (2008). Assessing integrated water management options for urban developments - Canberra case study. *Urban Water J.*, 5(2):147–159.

Statistics Canada (1988). Census tracts, Vancouver: part 2, profiles, 1986 census of Canada. Catalogue 95-168.

Stewart, I. D. and Oke, T. R. (2012). Local climate zones for urban temperature studies. *Bull. Amer. Meteor. Soc.*, 93(12):1879–1900.

Stull, R. B. (1988). *An Introduction to Boundary Layer Meteorology.* Springer Netherlands.

Sun, F., Roderick, M. L., Lim, W. H., and Farquhar, G. D. (2011). Hydroclimatic projections for the Murray-Darling Basin based on an ensemble derived from Intergovernmental Panel on Climate Change AR4 climate models. *Water Resour. Res.*, 47(12).

Swinbank, W. C. (1951). The measurement of vertical transfer of heat and water vapor by eddies in the lower atmosphere. *J. Meteor.*, 8(3):135–145.

Tabesh, M., Asadiyani Yekta, A. H., and Burrows, R. (2009). An integrated model to evaluate losses in water distribution systems. *Water Resour. Manag.*, 23(3):477–492.

Taylor, K. E. (2001). Summarizing multiple aspects of model performance in a single diagram. *J. Geophys. Res. Atmos.*, 106(D7):7183–7192.

Templeton, N. P., Vivoni, E. R., Wang, Z.-H., and Schreiner-McGraw, A. P. (2018). Quantifying water and energy fluxes over different urban land covers in Phoenix, Arizona. *J. Geophys. Res. Atmos.*, 123(4):2111–2128.

Tokarczyk, P., Leitao, J. P., Rieckermann, J., Schindler, K., and Blumensaat, F. (2015). High-quality observation of surface imperviousness for urban runoff modelling using UAV imagery. *Hydrol. Earth Syst. Sc.*, 19:4215–4228.

United Nations (2014). World urbanization prospects: the 2014 revision. Final Report ST/ESA/SER.A/366.

Uppala, S. M., Kållberg, P. W., Simmons, A. J., Andrae, U., Da Costa Bechtold, V., Fiorino, M., Gibson, J. K., Haseler, J., Hernandez, A., Kelly, G. A., Li, X., Onogi, K., Saarinen, S., Sokka, S., Allan, R. P., Andersson, E., Arpe, K., Balmaseda, M. A., Beljaars, A. C. M., Van De Berg, L., Bidlot, J., Bormann, N., Caires, S., Chevallier, F., Dethof, A., Dragosavac, M., Fisher, M., Fuentes, M., Hagemann, S., Hólm, E., Hoskins, B. J., Isaksen, L., Janssen, P. A. E. M., Jenne, R., McNally, A. P., Mahfouf, J.-F., Morcrette, J.-J., Rayner, N. A., Saunders, R. W., Simon, P., Sterl, A., Trenberth, K. E., Untch, A., Vasiljevic, D., Viterbo, P., and Woollen, J. (2005). The ERA-40 re-analysis. *Quart. J. Roy. Meteor. Soc.*, 131(612):2961–3012.

Valtanen, M., Sillanpää, N., and Setälä, H. (2014). Effects of land use intensity on stormwater runoff and its temporal occurrence in cold climates. *Hydrol. Process.*, 28(4):2639–2650.

Vickers, D. and Mahrt, L. (1997). Quality control and flux sampling problems for tower and aircraft data. *J. Atmos. Oceanic Technol.*, 14(3):512–526.

Ward, H. and Grimmond, C. (2017). Assessing the impact of changes in surface cover, human behaviour and climate on energy partitioning across Greater London. *Landscape Urban Plan.*, 165:142–161.

Ward, H. C., Järvi, L., Sun, T., Onomura, S., Lindberg, F., Olofson, F., Gabey, A., and Grimmond, C. S. B. (2017). Suews manual V2017b. Department of Meteorology, University of Reading, Reading, UK.

Ward, H. C., Kotthaus, S., Järvi, L., and Grimmond, C. S. B. (2016). Surface Urban Energy and Water Balance Scheme (SUEWS): development and evaluation at two UK sites. *Urban Climate*, 18:1–32.

Ward, H. C., Tan, Y. S., Gabey, A. M., Kotthaus, S., and Grimmond, C. S. B. (2018). Impact of temporal resolution of precipitation forcing data on modelled urban-atmosphere exchanges and surface conditions. *Int. J. Climatol.*, 36:649–662.

Weedon, G. P., Balsamo, G., Bellouin, N., Gomes, S., Best, M., and Viterbo, P. (2014). The WFDEI meteorological forcing data set: WATCH Forcing Data methodology applied to ERA-Interim reanalysis data. *Water Resour. Res.*, 50:7505–7514.

Weedon, G. P., Gomes, S., Viterbo, P., Österle, H., Adam, J. C., Bellouin, N., Boucher, O., and Best, M. (2010). The WATCH Forcing Data 1958–2001: a meteorological forcing dataset for land surface- and hydrological-models. WATCH Technical Report 22.

Weedon, G. P., Gomes, S., Viterbo, P., Shuttleworth, W. J., Blyth, E., Österle, H., Adam, J. C., Bellouin, N., Boucher, O., and Best, M. (2011). Creation of WATCH Forcing Data and its use to assess global and regional reference crop evaporation over land during the twentieth century. *J. Hydrometeorol.*, 12:823–848.

Weibull, W. (1939). A statistical theory of the strength of materials. *Ing. Vet. Ak. Handl.*, 151:1–45.

Wilby, R. L., Hay, L. E., Gutowski, W. J., Arritt, R. W., Takle, E. S., Pan, Z., Leavesley, G. H., and Clark, M. P. (2000). Hydrological responses to dynamically and statistically downscaled climate model output. *Geophys. Res. Lett.*, 27(8):1199–1202.

Wood, A. W., Leung, L. R., Sridhar, V., and Lettenmaier, D. P. (2004). Hydrologic implications of dynamical and statistical approaches to downscaling climate model outputs. *Climatic Change*, 62(1):189–216.

Wood, C. R., Järvi, L., Kouznetsov, R. D., Nordbo, A., Joffre, S., Drebs, A., Vihma, T., Hirsikko, A., Suomi, I., Fortelius, C., O'Connor, E., Moiseev, D., Haapanala, S., Moilanen, J., Kangas, M., Karppinen, A., Vesala, T., and Kukkonen, J. (2013). An overview of the urban boundary layer atmosphere network in Helsinki. *Bull. Amer. Meteor. Soc.*, 94(11):1675–1690.

Wood, C. R., Lacser, A., Barlow, J. F., Padhra, A., Belcher, S. E., Nemitz, E., Helfter, C., Famulari, D., and Grimmond, C. S. B. (2010). Turbulent flow at 190 m height above London during 2006–2008: A climatology and the applicability of similarity theory. *Bound.-Layer Meteor.*, 137(1):77–96.

World Meteorological Organization (2011). Guide to climatological practices. WMO-No. 100, World Meteorological Organization, Geneva.

World Meteorological Organization (2015). Status of the global observing system for climate. GCOS No. 195.

Wu, P., Ding, Y., and Liu, Y. (2017). Atmospheric circulation and dynamic mechanism for persistent haze events in the Beijing-Tianjin-Hebei region. *Adv. Atmos. Sci.*, 34:429–440.

Xia, X., Chen, X., Liu, R., and Liu, H. (2011). Heavy metals in urban soils with various types of land use in Beijing, China. *J. Hazard. Mater.*, 186(2):2043–2050.

Yufen, R., Xiaoke, W., Zhiyun, O., Hua, Z., Xiaonan, D., and Hong, M. (2008). Stormwater runoff quality from different surfaces in an urban catchment in Beijing, China. *Water Environ. Res.*, 80(8):719–724.

Zhang, Y., Grant, A., Sharma, A., Chen, D., and Chen, L. (2009). Assessment of rainwater use and greywater reuse in high-rise buildings in a brownfield site. *Water Sci. Technol.*, 60(3):575–581.

Zhao, B., Wang, S. X., Liu, H., Xu, J. Y., Fu, K., Klimont, Z., Hao, J. M., He, K. B., Cofala, J., and Amann, M. (2013). NO_x emissions in China: historical trends and future perspectives. *Atmos. Chem. Phys.*, 13(19):9869–9897.